A project report on

LUNGCRAFT: NAVIGATING LUNGS WITH 3D DIAGNOSTICS

Submitted in partial fulfillment for the award of the degree of

M.Tech. (Integrated) Computer Science and Engineering with Specialization in Business Analytics

by

NITHIN KODIPYAKA (20MIA1075)

VIT®
Vellore Institute of Technology
(Deemed to be University under section 3 of UGC Act, 1956)
CHENNAI

SCHOOL OF COMPUTER SCIENCE AND ENGINEERING

November, 2024

LUNGCRAFT: NAVIGATING LUNGS WITH 3D DIAGNOSTICS

Submitted in partial fulfillment for the award of the degree of

M.Tech. (Integrated) Computer Science and Engineering with Specialization in Business Analytics

by

NITHIN KODIPYAKA (20MIA1075)

VIT®
Vellore Institute of Technology
(Deemed to be University under section 3 of UGC Act, 1956)
CHENNAI

SCHOOL OF COMPUTER SCIENCE AND ENGINEERING

November 2024

VIT®

Vellore Institute of Technology

(Deemed to be University under section 3 of UGC Act, 1956)

CHENNAI

DECLARATION

I hereby declare that the thesis entitled "LUNGCRAFT: NAVIGATING LUNGS WITH 3D DIAGNOSTICS" submitted by me, for the award of the degree of M.Tech. (Integrated) Computer Science and Engineering with Specialization in Business Analytics, Vellore Institute of Technology, Chennai, is are cord of Bonafide work carried out by me under the supervision of DR. SUGANYA G.

I further declare that the work reported in this thesis has not been submitted and will not be submitted, either in part or in full, for the award of any other degree or diploma in this institute or any other institute or university.

Place: Chennai

Date: 10th November, 2024 **Signature of the Candidate**

VIT®

Vellore Institute of Technology

(Deemed to be University under section 3 of UGC Act, 1956)

CHENNAI

School of Computer Science and Engineering

CERTIFICATE

This is to certify that the report entitled **"LUNGCRAFT: NAVIGATING LUNGS WITH 3D DIAGNOSTICS"** is prepared and submitted by **Nithin Kodipyaka (20MIA1075)** to Vellore Institute of Technology, Chennai, in partial fulfillment of the requirement for the award of the degree of **M.Tech. (Integrated) Computer Science and Engineering with Specialization in Business Analytics** programme is a Bonafide record carried out under my guidance. The project fulfills the requirements as per the regulations of this University and in my opinion meets the necessary standards for submission. The contents of this report have not been submitted and will not be submitted either in part or in full, for the award of any other degree or diploma and the same is certified.

Signature of the Guide:

Name: Dr. Suganya G

Date: 10th November, 2024

Signature of the Examiner 1	Signature of the Examiner 2
Name: Dr. Brindha	Name: Dr. Suvidha Rupesh Kumar
Date:	Date:

Approved by the Head of Department

ABSTRACT

LungCraft is a new application of the advanced 3D modeling and visualization techniques for computed tomography (CT) scans to better lung cancer diagnosis. In this study, a detailed dataset from The Cancer Imaging Archive will be applied by diagnostic contrast-enhanced CT scans from 61 patients diagnosed with lung adenocarcinoma. In general, the objective is to evaluate prognosis more accurately by quantitatively analyzing how image features relate to the characteristics of tumors and their outcomes in patients. The two features implemented in this work were most critical to CT: intratumor heterogeneity and tumor shape complexity, systematically scored from routinely acquired diagnostic CT images. Such features allow distinct imaging phenotypes to be recognized and are associated with highly correlated survival differences. LungCraft applies static and interactive 3D visualizations to achieve a more intuitive presentation of the morphology of tumors in the better perception of tumor behavior than the traditional techniques applied with 2D imaging. The implementation is based on a hybrid modeling approach that balances machine learning algorithms designed for the analysis of CT scans with compensation for variation in clinical image acquisition. Our results show that the quantitative imaging features are reproducible and stable, thereby revalidating their potential as valuable tools for making diagnostic decisions on lung adenocarcinoma management. This work underscores the utility of 3D imaging as an adjunct to conventional diagnostic practices and possibly transforming the approach toward evaluation and management of lung cancer in the future. Future work will include refining these techniques and clinical evaluation to determine how they can be integrated into clinical workflows.

ACKNOWLEDGEMENT

It is my pleasure to express with deep sense of gratitude to Dr. Suganya G, Associate Professor Sr., School of Computer Science and Engineering, Vellore Institute of Technology, Chennai, for her constant guidance, continual encouragement, understanding; more than all, she taught me patience in my endeavor. My association with her is not confined to academics only, but it is a great opportunity on my part of work with an intellectual and expert in the field of Machine Learning.

It is with gratitude that I would like to extend my thanks to the visionary leader Dr. G. Viswanathan our Honorable Chancellor, Mr. Sankar Viswanathan, Dr. Sekar Viswanathan, Dr. G V Selvam Vice Presidents, Dr. Sandhya Pentareddy, Executive Director, Ms. Kadhambari S. Viswanathan, Assistant Vice-President, Dr. V. S. Kanchana Bhaaskaran Vice-Chancellor, Dr.T. Thyagarajan Pro-Vice Chancellor, VIT Chennai and Dr. P. K. Manoharan, Additional Registrar for providing an exceptional working environment and inspiring all of us during the tenure of the course.

Special mention to Dr. Ganesan R, Dean, Dr. Parvathi R, Associate Dean Academics, Dr. Geetha S, Associate Dean Research, School of Computer Science and Engineering, Vellore Institute of Technology, Chennai for spending their valuable time and efforts in sharing their knowledge and for helping us in every aspect.

In jubilant state, I express ingeniously my whole-hearted thanks to Dr.Sivabalakrishnan. M, Head of the Department, Project Coordinator, Dr. Yogesh C, SCOPE, Vellore Institute of Technology, Chennai, for their valuable support and encouragement to take up and complete the thesis.

My sincere thanks to all the faculties and staff at Vellore Institute of Technology, Chennai, who helped me acquire the requisite knowledge. I would like to thank my parents for their support. It is indeed a pleasure to thank my friends who encouraged me to take up and complete this task.

Place: Chennai

Date: **Nithin Kodipyaka**

CONTENTS

LIST OF FIGURES

LIST OF TABLES

LIST OF ACRONYMS

CT	Computed Tomography
CNN	Convolutional Neural Network
DICOM	Digital Imaging and Communications in Medicine
TCIA	The Cancer Imaging Archive
HU	Hounsfield Units
3D	Three-Dimensional
2D	Two-Dimensional

Chapter 1

Introduction

1.1 INTRODUCTION

Lung cancer stands as one of the leading causes of cancer-related deaths worldwide, with lung adenocarcinoma representing the most prevalent and aggressive subtype. Due to its high recurrence rate and complex growth patterns, lung adenocarcinoma presents significant challenges for early diagnosis and prognosis, critical factors for improving patient survival. Despite advancements in imaging technology, current diagnostic approaches—primarily two-dimensional (2D) computed tomography (CT) scans—fall short in capturing the intricate structural and density-based details of these tumors. The limitations inherent in 2D imaging, including a lack of spatial depth and difficulty in detecting intratumor heterogeneity, can lead to misinterpretation of tumor characteristics and suboptimal treatment decisions.

A major obstacle in diagnosing lung adenocarcinoma effectively is its morphological complexity and internal density variability. Traditional imaging techniques struggle to accurately represent these characteristics, which are crucial indicators for prognosis and therapy planning. Tumor shape complexity and density fluctuations, for example, have been associated with patient outcomes and disease progression. However, 2D CT scans provide minimal information on these dimensions, making it difficult for clinicians to evaluate the full extent of tumor aggressiveness and inform personalized treatment approaches.

This paper introduces LungCraft, an innovative framework designed to bridge these diagnostic gaps by offering three-dimensional (3D) modeling and interactive visualization capabilities for lung tumors. LungCraft leverages data from The Cancer Imaging Archive (TCIA), specifically the LungCT-Diagnosis collection, which includes CT scans from 61 patients with associated clinical metadata. This dataset enables comprehensive feature extraction, including tumor shape and density variations, providing a solid foundation for prognostic evaluation. By transforming CT scan data into high-resolution 3D models, LungCraft allows clinicians to examine tumors from multiple angles, thereby gaining deeper insights into morphological and density-based complexities that may influence clinical outcomes.

LungCraft aims to complement and extend traditional diagnostic tools by offering a dynamic and intuitive approach to lung cancer imaging, enabling improved accuracy in diagnosis and prognosis. Through interactive 3D visualization combined with quantitative feature scoring, LungCraft serves as a powerful tool for enhancing understanding of tumor behavior, potentially improving personalized treatment strategies for lung cancer patients.

1.2 CHALLENGES

Lung cancer is one of the leading causes of cancer-related deaths worldwide, accounting for more deaths than colon, breast, and prostate cancers combined. Among the different types of lung cancer, adenocarcinoma is particularly lethal due to its high recurrence rates and complex growth patterns. Early detection and precise diagnosis are crucial for improving patient survival; however, these goals are difficult to achieve with the current standard of care. While advances in imaging technology have enhanced lung cancer detection rates, accurate diagnostic methods that offer detailed insights into tumor morphology and density are still lacking. This underscores the need for innovative tools that can provide a more comprehensive understanding of lung tumors, thereby enabling personalized and effective treatment plans.

Lung cancer, particularly adenocarcinoma, presents a complex diagnostic challenge due to the high heterogeneity of tumor structures and their intricate growth patterns. Traditional diagnostic methods, primarily relying on 2D computed tomography (CT) scans, face several limitations that complicate accurate and early diagnosis:

- Limited Visualization of Tumor Complexity: Conventional 2D CT imaging restricts visualization to axial slices, making it difficult to appreciate the full spatial complexity of tumor shapes and intratumor heterogeneity. This limitation affects the ability to assess tumor boundaries, shape irregularities, and variations in density, which are critical for determining the malignancy and aggressiveness of tumors.
- Challenges in Capturing Prognostic Features: Key features, such as tumor shape complexity and density fluctuations within the tumor, are often lost in 2D imaging. Studies have shown that these features correlate with patient outcomes, but existing imaging modalities do not effectively quantify or visualize these attributes in a way that can reliably inform prognosis.
- Manual Interpretation and Inter-observer Variability: Diagnosing lung cancer through CT scans is typically a manual process that relies on radiologists' interpretations, leading to potential inconsistencies and inter-observer variability. The lack of standardized, quantitative imaging metrics further complicates diagnosis and treatment planning, especially in early-stage detection.
- Data and Computation Limitations in 3D Modeling: Before LungCraft, attempts to use 3D imaging and machine learning for lung cancer diagnosis faced challenges related to data processing and computational load. Many models struggled to handle large 3D datasets efficiently, leading to issues in segmentation accuracy, model generalizability, and computational feasibility for real-time applications.
- Integration of Machine Learning with Clinical Imaging: Machine learning models, while promising, have been challenging to implement directly in clinical settings due to data inconsistencies, lack of interpretability, and complex computational requirements. Creating a model that integrates seamlessly with clinical imaging workflows, while providing interpretable results, has been a major barrier.

1.3 PROJECT STATMENT

Lung Lung cancer remains one of the deadliest cancers worldwide, with late-stage detection significantly reducing survival rates. Despite advancements in imaging technology, current diagnostic approaches predominantly rely on 2D CT scans, which

are limited in their ability to represent the complex three-dimensional structure and heterogeneity of tumors. These limitations hinder the accurate assessment of tumor morphology, intratumor heterogeneity, and spatial relationships with surrounding tissues, which are essential for precise diagnosis, staging, and prognosis.

Additionally, there is a lack of quantitative tools that can systematically score and visualize tumor features in a way that correlates with clinical outcomes. Existing diagnostic methods also lack integration with machine learning models that could aid in automated classification and risk assessment, contributing to diagnostic delays and variability across radiologists. Given the computational demands and data processing challenges associated with 3D medical imaging, developing a scalable, clinically viable solution has been difficult.

Objective: This project aims to address these gaps by developing LungCraft, a 3D modeling and visualization framework that enhances lung cancer diagnosis through interactive, quantitative analysis of CT scans. By combining interactive 3D tumor visualization with machine learning classification models, LungCraft seeks to improve the accuracy of diagnostic assessments and provide clinicians with deeper insights into tumor characteristics, ultimately supporting better patient outcomes.

Key objectives of LungCraft include:

1. Interactive 3D Tumor Visualization: LungCraft will enable clinicians to interactively examine tumors in three dimensions, offering a more comprehensive view of tumor morphology and spatial positioning relative to nearby tissues. This 3D visualization allows for improved assessment of tumor size, shape, and heterogeneity, which are critical factors in staging and treatment planning.
2. Quantitative Analysis of Tumor Features: LungCraft aims to incorporate tools that systematically score and quantify tumor characteristics. By providing clinicians with objective metrics, this feature can standardize diagnostic criteria, reducing inter-observer variability and enhancing diagnostic accuracy.
3. Integration with Machine Learning Models: To further assist clinicians, LungCraft will integrate machine learning models for automated tumor classification and risk assessment. By leveraging ML algorithms, LungCraft can assist in differentiating between malignant and benign tumors, assessing tumor aggressiveness, and predicting likely clinical outcomes. This integration aims to support rapid and accurate diagnostic decision-making while minimizing subjective biases.
4. Scalable and Clinically Viable Design: A significant challenge in 3D medical imaging is balancing computational demands with clinical usability. LungCraft is designed to be scalable, enabling it to process high volumes of 3D imaging data in a way that is compatible with standard clinical workflows. By optimizing data processing and storage techniques, LungCraft seeks to bring advanced imaging and ML capabilities within reach of healthcare facilities, including those with limited computational resources.

1.4 OBJECTIVES

The LungCraft project is designed with the following objectives to enhance lung cancer diagnosis using 3D modeling and machine learning:

1. Develop a 3D Reconstruction Pipeline for CT Scans

The core of the LungCraft project is the 3D reconstruction pipeline, which is designed to process raw CT scan data into high-resolution 3D models. This pipeline will provide clinicians with an interactive, comprehensive visualization of lung anatomy and tumor morphology, transcending the constraints of traditional 2D imaging.

- Data Preprocessing: Begin by standardizing CT scan data to ensure consistency in image quality and format, removing noise and adjusting for image artifacts that could distort the 3D model.
- Segmentation of Lung Structures: Implement automated or semi-automated segmentation algorithms, such as U-Net-based architectures, to isolate lung tissue and tumor regions accurately. This step is essential for reconstructing clear, anatomically accurate 3D models.
- 3D Volume Reconstruction: Apply voxel-based modeling techniques to reconstruct CT slices into a volumetric 3D model. Techniques such as Marching Cubes or Surface Nets algorithms will be used to create high-fidelity models that retain critical details, including tumor shape, size, and position.
- Rendering for Interactivity: Render the 3D model in an interactive framework, allowing clinicians to manipulate the model dynamically, adjust views, zoom in on specific areas, and analyze the structure from various perspectives. By doing so, clinicians gain a more holistic view of the tumor and its relationship with surrounding tissues.

2. Enable Quantitative Feature Extraction of Tumor Characteristics

LungCraft will include a sophisticated quantitative analysis module to extract and score key prognostic features from CT scans. This module provides objective metrics on tumor characteristics, which are crucial for assessing tumor aggression and potential patient outcomes.

- Feature Extraction: Use image processing algorithms to quantify tumor-specific features. For example, shape complexity metrics (such as surface area-to-volume ratios or fractal dimension) provide insight into the irregularity of tumor boundaries, while heterogeneity metrics (such as texture analysis using Gray Level Co-occurrence Matrix (GLCM) or Local Binary Patterns (LBP)) capture variations in tissue density within the tumor.
- Morphological Analysis: Measure tumor size, volume, and spatial orientation to assess growth patterns and their possible impact on adjacent tissues. This information can help correlate imaging findings with clinical behaviors, supporting prognostic assessments.
- Data Correlation with Clinical Outcomes: Integrate these quantitative features with anonymized clinical data (such as patient survival rates or recurrence patterns) to establish correlations between imaging phenotypes and patient outcomes. This will

aid in developing predictive models that can provide clinicians with valuable insights into the likely progression of individual cases.

3. Implement Advanced Machine Learning Models for Tumor Classification

LungCraft will leverage machine learning to classify lung tumors and predict their characteristics, thereby automating key aspects of the diagnostic process and enhancing classification accuracy.

- HybridNET Architecture: Deploy a hybrid convolutional neural network (CNN) model that combines 3D CNN layers for volumetric analysis with 2D convolutional layers for feature extraction from individual CT slices. This hybrid approach capitalizes on both spatial and texture information to improve classification performance.
- Model Training: Use labeled datasets of lung CT scans, including both benign and malignant cases, to train the model. Data augmentation techniques will enhance the robustness of the model by simulating variations in tumor morphology and appearance, helping it generalize to diverse cases.
- Classification Outputs: The model will output a probabilistic assessment of tumor malignancy, along with predictions about specific tumor characteristics (e.g., size, density). These outputs are designed to support radiologists in making accurate, rapid decisions based on standardized criteria.
- Explainability and Transparency: Incorporate techniques such as Grad-CAM (Gradient-weighted Class Activation Mapping) to highlight image regions that contributed to the model's predictions, ensuring clinicians have insight into the model’s decision-making process, which is essential for clinical adoption.

4. Enhance Diagnostic Visualization Through Interactive 3D Modeling

Interactive visualization is crucial for improving diagnostic insights, enabling clinicians to examine the tumor in relation to the surrounding anatomy dynamically. LungCraft will incorporate a specialized interactive visualization module that allows intuitive exploration of 3D tumor models.

- Dynamic Manipulation Tools: Clinicians will be able to rotate, zoom, and slice through the 3D model. This functionality provides a more immersive view, aiding in understanding tumor behavior, growth patterns, and relationships with critical structures (e.g., bronchi, blood vessels).
- Annotations and Markup Capabilities: Enable clinicians to annotate specific regions of interest within the model, such as points of high heterogeneity or critical boundaries. This feature supports collaborative diagnoses and detailed analysis, with annotations shared across the care team as needed.
- Real-Time Feature Highlighting: Integrate the quantitative feature extraction results into the visualization, allowing for real-time overlay of metrics (e.g., shape complexity, density gradients). These visual aids facilitate the rapid assessment of tumor attributes, supporting decisions around biopsy locations or surgical interventions.

5. Ensure Clinical Feasibility and Efficiency

To ensure LungCraft's utility in clinical environments, the project emphasizes the importance of computational efficiency, seamless integration into existing workflows, and scalability.

- Optimization of Computational Load: Use parallel processing and optimized algorithms to accelerate 3D reconstruction and feature extraction, ensuring that LungCraft operates efficiently even with high-resolution datasets.
- Workflow Integration: Design the system to be compatible with standard clinical imaging software and PACS (Picture Archiving and Communication System) platforms. A user-friendly interface with a minimal learning curve is prioritized to facilitate widespread clinical adoption.
- Scalability and Cloud Compatibility: Provide the option for cloud-based processing, enabling LungCraft to handle large-scale data processing needs and making it accessible to clinics with varying levels of computational resources. This cloud compatibility supports scalability, allowing the tool to be utilized across multiple clinical sites without requiring extensive local infrastructure

1.5 SCOPE OF THE PROJECT

The LungCraft project is designed to address critical limitations in lung cancer diagnosis by integrating advanced 3D imaging and machine learning capabilities within a unified framework. The project involves developing a comprehensive pipeline for processing and reconstructing CT scan data into detailed 3D models, specifically focused on visualizing lung anatomy and tumor morphology. By standardizing image data across varying acquisition protocols and resolutions, LungCraft ensures consistency in 3D reconstructions, enabling an accurate representation of anatomical structures within the lungs.

This project further aims to provide quantitative imaging insights through the extraction of key tumor features, including shape complexity and intratumor heterogeneity, which are significant for prognostic evaluations. These quantitative metrics, derived from high-resolution 3D models, enhance traditional diagnostic approaches by offering deeper insights into tumor characteristics that correlate with patient outcomes. Additionally, LungCraft incorporates machine learning models, including a hybrid 3D CNN architecture, to automate the classification of lung cancer presence and severity based on these imaging phenotypes. This integration of 3D visualization and predictive analytics aims to streamline diagnostic workflows and reduce inter-observer variability, offering a more robust and standardized tool for lung cancer assessment.

LungCraft is ultimately designed with clinical application in mind, balancing computational efficiency with diagnostic effectiveness to facilitate smooth integration into real-world healthcare environments. The project focuses on creating a practical and scalable solution that can support radiologists and oncologists in making more accurate and timely diagnoses, potentially improving treatment planning and patient outcomes in lung cancer care.

Chapter 2

Related Work

Gerckens et al. (2019) developed 3D lung tissue cultures (3D- LTCs) from precision-cut lung slices (PCLS) to model human lung diseases more effectively. Their work emphasizes the importance of preserving tissue architecture, biomechanics, and cellular diversity to closely resemble in situ lung conditions. The 3D-LTCs enable detailed analysis of drug responses and disease mechanisms, particularly in fibrosis research, offering personalized insights through patient- derived tissue. While their focus lies on ex vivo modeling for biochemical studies, our research diverges by using non- invasive CT-based 3D models to visualize tumor structures and predict patient outcomes. Both studies contribute to advancing personalized medicine, with Gerckens et al. providing tissue-level insights and our work focusing on diagnostic imaging for improved lung cancer prognosis [1].

Alakwaa et al. (2017) introduced a computer-aided diagnosis (CAD) system leveraging 3D convolutional neural networks (3D-CNNs) for lung cancer detection using CT scans. Their approach focuses on automating the segmentation, detection, and classification processes by integrating a modified U-Net and 3D-CNNs. Although the use of deep learning in their work yields a high classification accuracy of 86.6%, it also highlights the challenges of false positives during nodule detection. While their research centers on the application of machine learning models to automate cancer diagnosis, our work shifts toward enhancing diagnostic visualization through interactive 3D models of CT scans. Both studies aim to improve lung cancer management, but ours focuses on combining imaging phenotypes and survival analysis to offer a more interpretable, non-invasive approach for clinical applications [2].

Cunniff et al. (2021) explored the development and visualization of lung organoids, emphasizing the importance of maintaining the 3D architecture of lung tissue for accurate biological modeling. Their work highlights how conventional 2D culture systems fail to capture the complexity of lung structures, which is essential for understanding disease mechanisms. By leveraging high-resolution microscopy, they demonstrate how lung organoids can replicate in vivo conditions, offering insights into both healthy and diseased states of the lung. While their research focuses on 3D tissue cultures for experimental manipulation, our study extends the idea of 3D modeling by applying it directly to diagnostic CT scans, enabling clinicians to visualize tumor heterogeneity and shape complexity interactively. Both efforts underscore the critical role of 3D visualization in advancing lung disease research and treatment strategies [3].

Uhl et al. (2015) developed and validated patient-derived 3D lung tissue cultures (LTCs) to investigate Wnt/β-catenin signaling for lung tissue repair, focusing on chronic obstructive pulmonary disease (COPD). Their work emphasizes the importance of mimicking the native lung microenvironment through 3D models, which allow for detailed molecular analysis and high-resolution imaging. They demonstrated the activation of Wnt/β-catenin signaling pathways in patient-derived tissues, showing promising therapeutic potential through enhanced epithelial cell regeneration and reduced tissue degradation. While their study focuses on preclinical therapeutic validation for COPD, it aligns with our work's goal of leveraging 3D visualization for diagnostic and therapeutic advancements. Both approaches highlight the utility of 3D models in advancing personalized healthcare by closely replicating patient- specific lung environments [4].

Tan and Liu (2021) introduced a novel framework that combines 3D CNNs with BERT for the automatic diagnosis of COVID-19 from CT scan images. Their approach involves preprocessing CT slices by segmenting lung regions and filtering out irrelevant backgrounds. A resampling method ensures consistent input size by selecting a fixed number of slice images for training and validation. The framework uses a 3D CNN to extract spatial features, integrated with BERT to enhance contextual understanding of the images. The extracted features are aggregated into a feature vector and fed into a multi-layer perceptron (MLP) for final classification. Their model achieved high performance, with an F1 score of 0.9261 on validation and 0.8822 on test datasets. This work demonstrates the effectiveness of combining deep learning models with language models for image-based medical diagnosis, which aligns with our use of 3D data but emphasizes COVID-19 detection. The framework showcases the potential of 3D models for diagnostic applications, further motivating our exploration of 3D visualization for lung cancer analysis [5].

Ikeda et al. (2013) highlighted the value of three-dimensional (3D) computed tomography (CT) lung modeling in enhancing the precision and safety of lung cancer surgeries. With the rise of minimally invasive procedures, such as video-assisted thoracoscopic surgery (VATS) lobectomy and segmentectomy, understanding the complex anatomy of pulmonary vessels and bronchi is critical for successful operations. The use of multi-detector CT (MDCT) allows surgeons to generate detailed 3D images of lung structures, enabling preoperative simulations and real-time navigation during surgery. This technology provides surgeons with a comprehensive view of vascular and bronchial pathways, enhancing both the accuracy of dissections and patient safety. Advances in imaging software have further improved the visualization of small vessels, supporting more precise segmentectomy procedures. Ikeda et al. emphasize that 3D modeling not only facilitates safer surgeries but also serves as a valuable tool for training junior surgeons and boosting operator confidence. This approach aligns with our focus on leveraging 3D

visualization to provide more detailed insights into lung structures, reinforcing the potential for improved medical interventions through advanced modeling techniques [6].

Cheng et al. (2016) explored the transformative impact of three-dimensional (3D) printing and 3D slicer technology in understanding and treating structural lung diseases. As the 3D printing industry advances, clinicians have begun to leverage these technologies for various applications, including pre- procedural planning, biomedical tissue modeling, and the production of custom implantable devices. However, the authors note that despite the growing adoption of rapid prototyping and additive manufacturing techniques in healthcare, many physicians still lack the necessary technical skills to utilize these innovative tools effectively. They discuss the rapid growth of the 3D printing sector, which introduces a multitude of 3D printers and materials, emphasizing the need for clinicians to remain informed about these developments to fully exploit their potential benefits. The paper reviews the history of 3D printing and its recent biomedical applications while addressing the significant barriers to its widespread adoption in the medical field. Cheng et al. also provide a guide for clinicians on designing personalized airway prostheses using 3D Slicer, aiming to facilitate greater participation in the 3D printing sector. This work underscores the importance of integrating advanced technologies into clinical practice, aligning with our objective of enhancing lung cancer diagnosis through innovative modeling and visualization techniques [7].

Dillavou et al. (2003) conducted a study to evaluate the accuracy of aortic diameter measurements using two- dimensional (2D) versus three-dimensional (3D) computed tomography (CT) scans. The research involved two independent, blinded observers who measured the aortic neck and sac diameters from 40 2.5-mm 2D CT scans of 31 patients using electronic calipers and a circular tool for 3D reconstructions. The measurements were obtained at specified anatomical landmarks, with data analyzed through intraclass correlation coefficients (ICC), Bland-Altman variation assessments, and absolute differences. The results indicated a high correlation between 2D minor axis measurements and 3D measurements, with the ICC values for the neck and sac demonstrating strong reliability (neck ICC = 0.9282; sac ICC = 0.8956). While the correlation for the major axis was lower, the average absolute difference between 3D and 2D minor axis diameters was just 1.01 mm, compared to 2.61 mm for the major axis. The authors concluded that minor axis measurements derived from 2D scans are generally sufficient for clinical applications, suggesting that 3D reconstructions may not be necessary for routine aortic diameter assessments. This study highlights the potential for simpler imaging techniques in clinical practice while also setting a foundation for the exploration of more advanced imaging methods, such as 3D modeling, in lung cancer diagnosis [8].

Kumar and Vijai (2012) discuss advancements in 3D reconstruction techniques of the human face from 2D CT scan images, emphasizing their applications in craniofacial surgery. The authors propose a software tool designed to aid surgeons in planning and

executing facial reconstruction procedures. They analyze various existing approaches for 3D reconstruction, which range from applications in visualizing real-world scenarios to modeling anatomical structures. The paper evaluates different algorithms, highlighting their suitability for reconstructing various regions of the face, including soft tissues and hard bones. The survey concludes by assessing the effectiveness of each method and recommending the most appropriate approaches for specific medical applications, underscoring the importance of precise modeling in improving surgical outcomes. This work contributes to the growing field of 3D imaging and modeling in medicine, which has significant implications for surgical planning and patient care [9].

Duquette et al. (2012) developed a semi-automatic method for 3D segmentation of the abdominal aorta, focusing on the aneurismal sac of abdominal aortic aneurysms (AAAs) from both CT and MR images. Utilizing graph cut theory, the method minimizes human intervention while effectively segmenting the lumen interface and aortic wall. Tested on a dataset of 44 patients and 10 synthetic images, the segmentation results were compared to manual tracings from four experts, demonstrating that the semi-automatic method achieved similar variability to human operators. This approach provides reliable and reproducible evaluations of the abdominal aorta, enhancing diagnostic accuracy and treatment planning for AAAs [10].

Kabadi et al. (2019) developed a novel 3D lung microtissue model to study nanoparticle-induced alterations in cell- matrix interactions, particularly focusing on multi-walled carbon nanotubes (MWCNTs). Traditional toxicity testing methods rely heavily on 2D in vitro assays and in vivo animal studies, which often yield conflicting results. In contrast, this study co-cultured human lung fibroblasts and epithelial cells with macrophages to form scaffold-free 3D microtissues, which more accurately mimic human physiology. After exposing these microtissues to MWCNTs, carbon black nanoparticles, and crocidolite asbestos fibers, the researchers evaluated microtissue viability, morphology, and gene expression associated with inflammation and extracellular matrix remodeling. The findings indicate that 3D lung microtissues can effectively predict chronic pulmonary endpoints and provide a more relevant alternative for nanomaterial toxicity testing, enhancing understanding of toxicity pathways and potential health hazards from nanoparticle exposure [11].

Subburaj, Ravi, and Agarwal (2009) present a novel computer graphics-based method for the automated identification of anatomical landmarks on 3D bone models reconstructed from CT scan images. The accurate localization of these landmarks is critical for patient-specific preoperative planning, such as tumor referencing and implant alignment, as well as for intra-operative navigation. The authors' method segments the bone model's surface into different landmark regions—peak, ridge, pit, and ravine—based on

surface curvature, and employs an iterative process using a spatial adjacency relationship matrix to label these regions automatically. The performance of the automated system was evaluated against manual landmark identification by three experienced orthopedic surgeons on three 3D bone models, revealing variability in landmark location ranging from 2.15–5.98 mm for the manual method and 1.92–4.88 mm for the automated approach. The results indicate that the automated methodology performed comparably or better than manual identification, demonstrating reproducibility and potential for various applications in surgical planning and navigation [12].

El-Baz et al. (2013) present a novel algorithm for the automatic detection of lung nodules in chest spiral low-dose CT (LDCT) scans, addressing a significant challenge in the computer analysis of chest radiographs. The proposed method involves three main steps: first, it isolates lung nodules, arteries, veins, bronchi, and bronchioles from surrounding anatomical structures. The second step utilizes deformable 2D and 3D templates that characterize the typical geometry and gray-level distribution of lung nodules for detection. This detection process combines normalized cross- correlation template matching with a genetic optimization algorithm to enhance accuracy. In the final step, the algorithm reduces false positives by applying three robust features to distinguish true lung nodules. Testing on 200 CT datasets demonstrates that the proposed algorithm achieves results comparable to those of expert radiologists, highlighting its potential utility in clinical practice for improving lung nodule detection accuracy [13].

Anwar (2021) discusses an innovative approach to diagnosing COVID-19 using AutoML techniques applied to 3D CT scans. The study highlights the limitations of polymerase chain reaction (PCR) tests, which have a high false-negative rate, necessitating alternative diagnostic methods. CT scans provide detailed insights into the chest but typically involve analyzing hundreds of slices, making manual diagnosis by radiologists and pulmonologists time- consuming. To address this, the author proposes an automated AI-based method that leverages AutoML for efficient diagnosis. The model is trained on 2D slices of CT scans rather than 3D scans, with predictions aggregated to label the overall 3D CT scan based on the most frequently occurring diagnosis among the slices. By employing different thresholds, the model classifies scans as COVID-positive or negative. The approach achieved an impressive accuracy of 89% and an F1-score of 88%, demonstrating its potential as a reliable diagnostic tool. The implementation is publicly available, contributing to further research and application in the clinical setting [14]

Serte and Demirel (2021) present a deep learning approach for diagnosing COVID-19 using 3D CT scans, addressing the urgent need for efficient detection methods in hospitals. With the rapid spread of COVID-19 and its associated mortality, timely isolation of infected individuals is crucial. CT scans serve as valuable diagnostic tools, but the extensive number of slices in each scan can cause delays in diagnosis. To overcome this challenge, the authors propose an AI-based methodology utilizing the ResNet-50 deep

learning model to classify CT images as either COVID-19 positive or normal. The model processes individual images from the 3D CT scans and aggregates these image-level predictions to provide a comprehensive diagnosis for the entire volume. The results indicate that this deep learning approach achieves an impressive area under the curve (AUC) value of 96%, demonstrating its potential effectiveness in rapid and accurate detection of COVID-19 from CT imaging [15].

Chapter 3

Dataset

In this study, we utilized a comprehensive dataset from The Cancer Imaging Archive (TCIA), as illustrated in Fig. 1. The dataset specifically comprises the LungCT-Diagnosis collection, a well-curated repository of diagnostic, contrast-enhanced CT scans of lung adenocarcinoma patients. This dataset underpins the development and evaluation of our AI-driven diagnostic tools, facilitating in-depth analysis of lung tumors for improved prognostic accuracy.

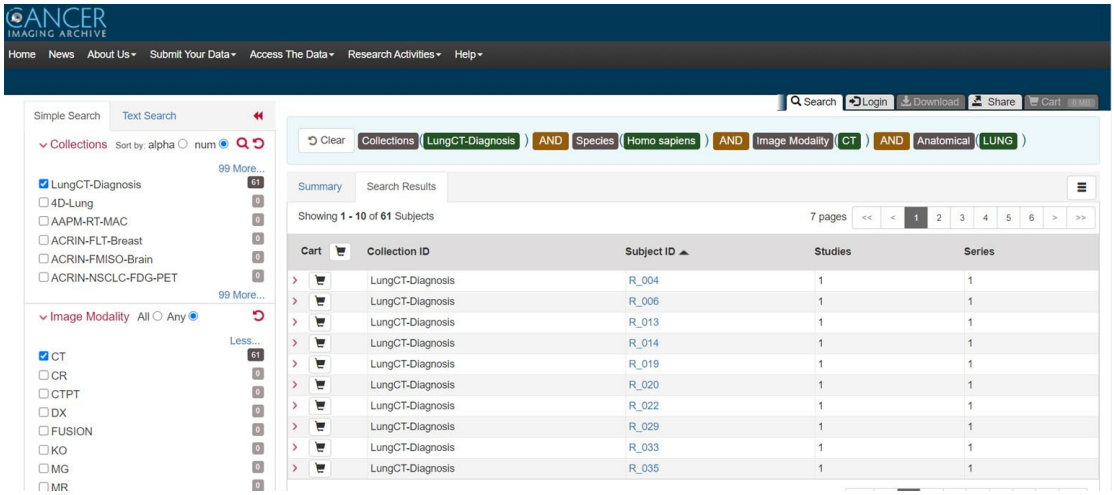

Figure 1 LungCT-Diagnosis dataset from Cancer Imaging Archive.

3.1 DATA OVERVIEW

Title: Quantitative Computed Tomographic Descriptors Associate Tumor Shape Complexity and Intratumor Heterogeneity with Prognosis in Lung Adenocarcinoma

DOI: 10.7937/K9/TCIA.2015.A6V7JIWX

Location: Lung

Species: Human

Subjects: 61 patients

Data Types: CT images and supporting clinical data

Cancer Types: Lung Cancer

Size: 2.47 GB

Status: Public, Complete

This dataset serves as a valuable resource for extracting imaging biomarkers related to tumor morphology and density variation. As lung adenocarcinoma has unique structural and density characteristics that correlate with prognosis, this data enables the development of robust, quantitative tools for tumor analysis and survival prediction.

3.2 DATASET SUMMARY

The **LungCT-Diagnosis collection** contains a total of 4,682 diagnostic contrast-enhanced CT images (see Fig. 2) obtained retrospectively. Each CT scan was acquired with slice thicknesses between 3 mm and 6 mm, standard for clinical imaging protocols. The images were retrospectively collected to ensure that patients had adequate follow-up before surgical intervention, allowing for a more accurate assessment of long-term survival outcomes.

The dataset's main purpose is to enable prognostic feature extraction, focusing on the identification and quantification of imaging markers that describe lung adenocarcinoma. Two essential quantitative features were developed:

1. Tumor Shape Complexity: Evaluates the irregularities in tumor contours and volume.
2. Intratumor Density Variation: Measures the fluctuations in density within the tumor, reflecting heterogeneity in cellular structure.

Both features are reproducible and show robustness across various clinical imaging protocols. Their stability despite differences in image acquisition parameters suggests that they could be integrated into routine diagnostic workflows for lung cancer management, providing valuable insights into patient outcomes.

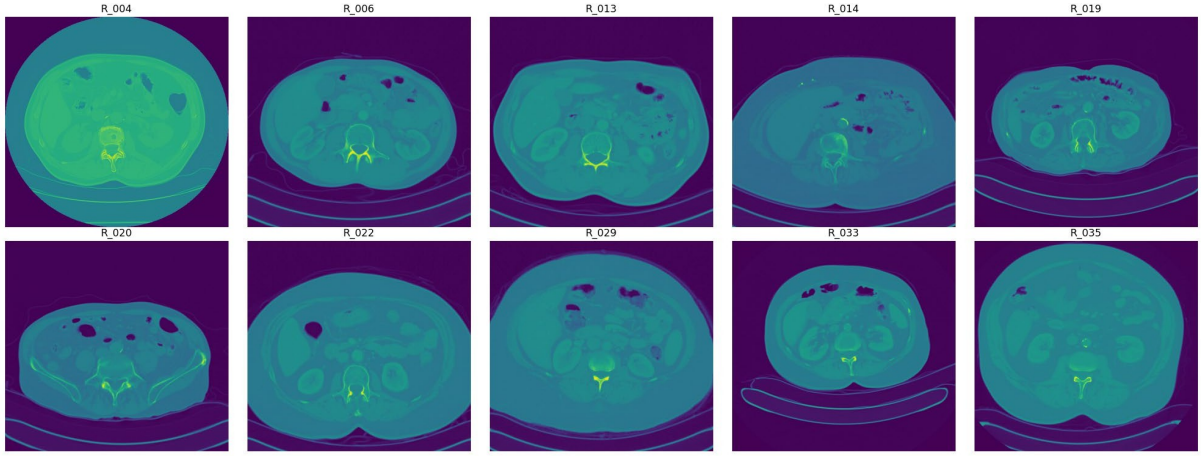

Figure 2 Visualization of raw DICOM files of different subjects

3.3 DATA ACCESS

The LungCT-Diagnosis dataset is publicly accessible via the TCIA platform. The data includes:

- CT Images: Available in DICOM format (2.47 GB).
- DICOM Metadata Digest: Provided in CSV format for easy reference.
- Representative Tumor Slices: Offered in XLS format to streamline analysis.
- Clinical Data: Available in DOC format for comprehensive patient profiles.

Access to this data requires the NBIA Data Retriever tool, which facilitates the downloading of large DICOM datasets from TCIA. Researchers must adhere to the TCIA Data Usage Policy, ensuring appropriate citation and compliance with data-sharing protocols.

3.4 DICOM FORMAT AND HOUNSFIELD UNITS

The DICOM (Digital Imaging and Communications in Medicine) format is the universal standard for storing, managing, and transferring medical imaging data, supporting interoperability across various imaging devices and software. Each DICOM file contains a series of cross-sectional slices of the patient's anatomy, with metadata detailing patient demographics and imaging parameters.

Within DICOM files, Hounsfield Units (HU) are employed to represent tissue density values. Calculated based on X-ray attenuation, HU values allow clinicians to differentiate between various tissues and structures. For instance, tumors display unique HU patterns that can assist in identifying abnormal growths. This dataset uses the .dcm extension for DICOM files, organizing them within folders named according to patient IDs. Each folder contains multiple CT slices, offering a detailed, multi-angled view of lung structures.

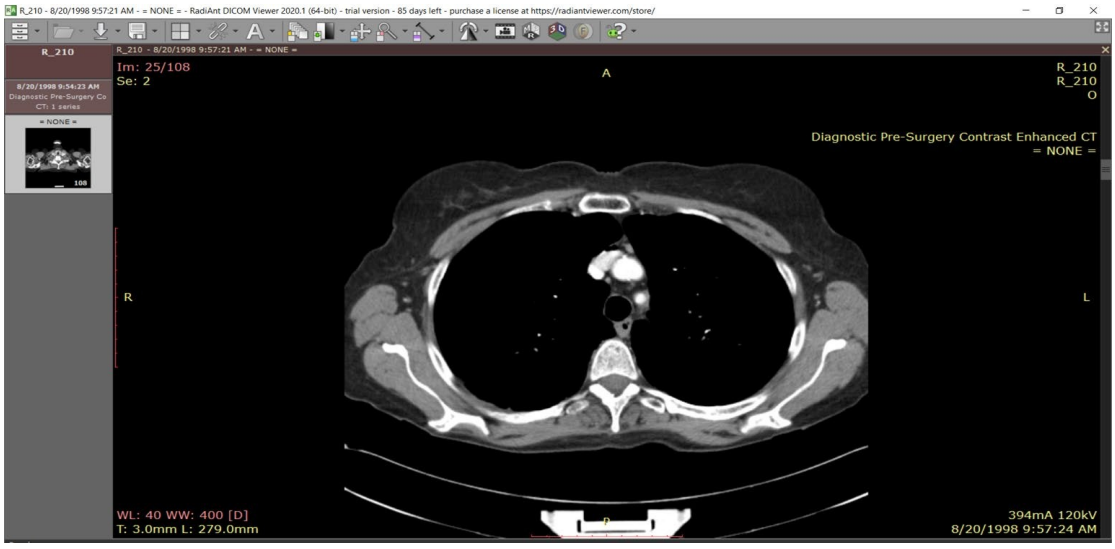

Figure 3 Visualization of a slice of CT scan of the subject R_210 showing raw metadata attached to it.

To simplify analysis, patients are categorized based on survival status—either ALIVE (1) or DEAD (0)—providing a binary classification for outcome prediction. Fig. 3 illustrates a sample DICOM file structure, showing how these files enable precise, layered imaging across varied anatomical perspectives.

Due to variation in the number of slices per patient folder, diverse clinical scenarios are captured, reflecting real-world variability in imaging protocols. Tools such as QuPath and Radiant DICOM Viewer were utilized for visualization and analysis, enhancing our understanding of tumor morphology and potential pathologies present in the scans.

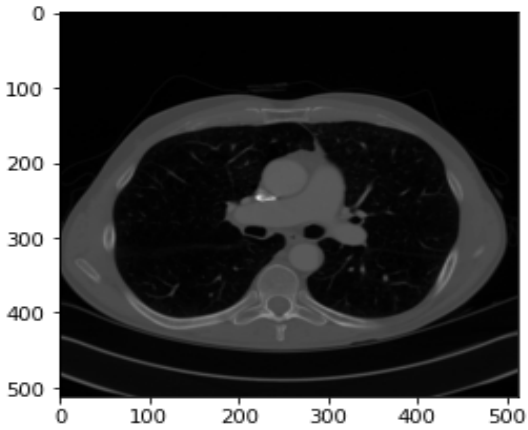

Figure 4 DICOM Slice visualized without DICOM Viewer using pydicom

3.5 PREPROCESSING PIPELINE

To ensure data consistency and enhance model performance, a series of preprocessing steps were implemented:

- Normalization: Pixel intensity values were normalized across scans (see Fig. 5), creating a standardized range to facilitate consistent analysis. Normalization minimizes the effects of lighting and contrast variations, enabling more accurate feature extraction.

- Resampling: Voxel dimensions were resampled to 1mm x 1mm x 1mm, standardizing spatial resolution across all scans. This resampling ensures uniformity, which is essential for comparing tumors across different patients and imaging sessions.

- Segmentation: Using Hounsfield Units (HU), lung regions were segmented to isolate the relevant anatomical structures. By focusing solely on lung tissue, segmentation improves computational efficiency and accuracy in identifying tumors and analyzing their features.

- Augmentation: Data augmentation techniques, including rotation, flipping, and noise addition, were applied to diversify the training dataset (Fig. 6). These augmentations increase model robustness, helping the model generalize better to new, unseen data by simulating variations in tumor appearance and orientation.

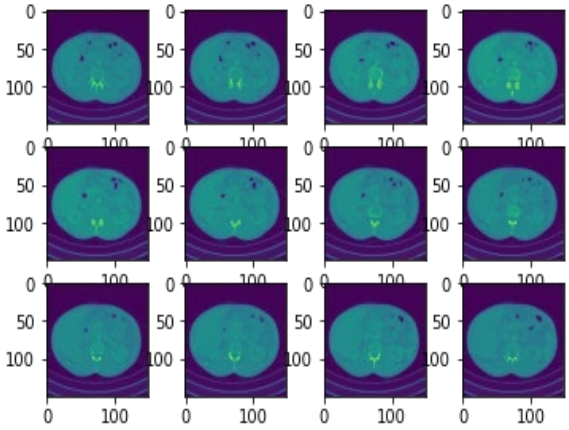

Figure 5 Data before preprocessing techniques.

3.6 ANNOTATION AND LABELING

Each CT scan is meticulously annotated with labels to indicate the presence or absence of lung adenocarcinoma. The annotations also include critical clinical information such as survival status and TNM staging (tumor-node-metastasis classification).

Annotations were conducted by experienced radiologists, ensuring high-quality and reliable data labels for training AI models. This comprehensive labeling provides a solid foundation for supervised learning, where models can learn to associate imaging features with specific diagnostic and prognostic outcomes.

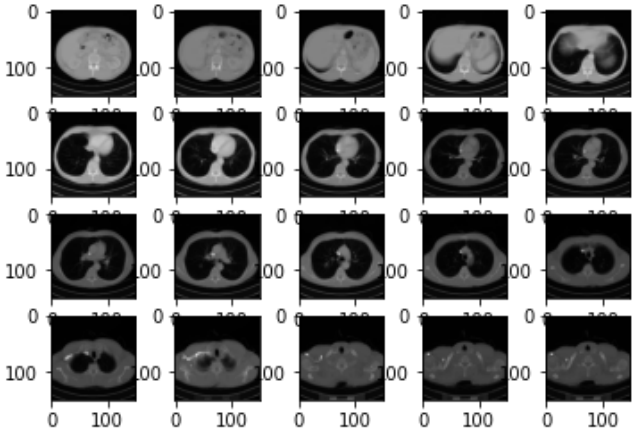

Figure 6 Data after preprocessing techniques

Chapter 4

Methodology

The architecture of this project is organized into four primary components, each designed to handle specific stages within the diagnostic pipeline: 3D image processing, lung segmentation and visualization, tumor localization, and machine learning for diagnosis. Each component applies distinct algorithms and frameworks to process medical images and contribute to a cohesive diagnostic model.

The pipeline starts by loading and preprocessing lung CT scans in Digital Imaging and Communications in Medicine (DICOM) format. These scans, consisting of multiple axial slices per patient, are processed using Python's pydicom library to create a standardized 3D voxel grid for further analysis.

4.1 3D IMAGE PROCESSING

Input: Lung CT scans in DICOM format
Processing: Sorting slices, converting pixel intensities to Hounsfield Units, and resampling to a consistent voxel size
Output: Preprocessed 3D voxel grid for further analysis

The pipeline begins with the acquisition of lung CT scans, formatted in DICOM (Digital Imaging and Communications in Medicine), which is the standard format for medical imaging data. Each CT scan comprises multiple axial slices for each patient.
The pydicom library is employed to load and preprocess these DICOM files, ensuring they are organized and standardized for subsequent analysis.

Slice Sorting and Hounsfield Unit Conversion

1. Sorting Slices: Each DICOM slice is organized based on the ImagePositionPatient tag to maintain the correct anatomical sequence. This step preserves the natural spatial ordering of slices for accurate 3D reconstruction.
2. Conversion to Hounsfield Units (HU): Each pixel intensity is converted to Hounsfield Units using the formula:

$$HU = pixel\_value \times RescaleSlope + RescaleIntercept$$

where RescaleSlope and RescaleIntercept are derived from the DICOM metadata. The HU scale represents tissue density, allowing the model to distinguish between air, lung tissue, and other structures.

Resampling to Uniform Spacing: To ensure consistency across scans, the images are resampled to an isotropic resolution of 1mm x 1mm x 1mm using cubic interpolation with scipy.ndimage.zoom. The new shape of each scan volume is calculated as follows:

$$new\_shape = (new\_spacing / old\_spacing) * old\_shape$$

This resampling standardizes the spatial resolution, allowing uniform analysis across all 3D scans.

Algorithm 1 Marching Cube Algorithm for 3D Lung Visualisation

Input:
scalarField: 3D array of scalar values (e.g., lung data)
isovalue: scalar value to extract the surface

Output:
triangles: list of triangles representing the extracted surface

Method:
1. Initialize *triangles* as an empty list.
2. **For** each voxel in *scalarField*:
   a. Calculate *cubeIndex* using *calculateCubeIndex(voxel, isovalue).*
   b. **For** each triangle in *getTriangleConfiguration(cubeIndex):*
      i. **If** triangle is valid:
         A. Interpolate vertices using *interpolateTriangleVertices(voxel, triangle, isovalue).*
         B. Add vertices to *triangles*.
3. Return *triangles*.

4.2 3D LUNG SEGMENTATION

Input: Preprocessed 3D voxel grid
Processing: Thresholding, morphological operations, and region-growing
Output: Binary mask of lungs, converted to a 3D mesh using Marching Cubes

The next phase focuses on segmenting the lung tissue, isolating it from other anatomical structures. Segmentation provides a focused area for tumor analysis and visualization [7].

Table 1 Hounsfield Unit Range for different Tissue type

Tissue Type	Hounsfield Unit (HU) Range	Description
Air	-1005 to -995	Lowest HU values, indicating the least dense material.
Lung	-950 to -550	Low HU values, representing air-filled spaces in the lungs.
Fat	-100 to -80	Relatively low HU values, indicating low tissue density.
Water	-4 to 4	Neutral HU value, representing the density of water.
Kidney	20 to 40	Moderate HU values, suggesting a denser tissue than water.
Pancreas	30 to 50	Slightly higher HU values compared to the kidney.
Blood	50 to 60	Moderately high HU values, indicating a denser tissue.
Muscle, Soft Tissue	20 to 100	A wide range of HU values, representing various soft tissues.
Liver	50 to 70	Relatively high HU values, indicating a denser tissue.
Adipose Tissue	-200 to -20	Lower HU values compared to other tissues, representing fat.
Spongious Bone	50 to 300	Higher HU values, indicating a denser tissue than soft tissues.
Compact Bone (Cortical)	>300	Highest HU values, representing the densest tissue in the body.

Thresholding and Morphological Operations

Segmentation of lung tissue is based on thresholding in Hounsfield Units (HU). Lung tissue typically falls within the HU range of -950 to -550 HU [3], while other tissues such as bone exhibit much higher values. Morphological operations are then applied to refine the lung mask:

- Erosion and Dilation: These operations remove small, isolated components and close gaps within the lung region.
- Region-Growing: This technique refines the segmented lung volume, specifically excluding structures like the heart and major blood vessels.

3D Visualization using Marching Cubes

Using the Marching Cubes algorithm, the binary lung mask is converted into a 3D surface mesh. Marching Cubes identifies surface boundaries within the voxel grid, creating a triangulated mesh that visualizes the lung's contours (see Table 1 for Hounsfield Unit thresholds by tissue type). This 3D visualization provides clinicians with an intuitive representation of lung structures.

4.3 3D TUMOR LOCALIZATION (INTERACTIVE)

- Input: Segmented lung and tumor metadata
- Processing: Mapping tumor coordinates from real-world to voxel space, overlaying tumor on lung segmentation
- Output: 3D visualization of lung with tumor location marked

This stage maps the tumor's location from clinical metadata onto the segmented 3D lung volume, allowing precise visualization of the tumor within the lung.

Tumor Position Mapping

Tumor coordinates, provided in real-world (millimeter) space, are transformed into voxel coordinates within the CT scan using the following equation:

$$voxel\_position = (real\_world\_position - origin) \,/\, voxel\_spacing$$

4.4 ML CLASSIFICATION

The final component of our methodology involves using a 3D Convolutional Neural Network (CNN) to classify lung scans based on disease presence [2].

Image Preprocessing: Each CT scan is resized to a fixed size of 150x150 pixels per slice, and the number of slices is standardized to 20 per patient to ensure uniform input dimensions. This preprocessing ensures that each patient's scan can be processed by the CNN consistently.

Input: Preprocessed CT scans (150x150 pixels, 20 slices per patient).

3D CNN Architecture:

- Convolutional Layers: Capture volumetric features.
- Pooling Layers: Reduce dimensionality while retaining key spatial information.
- Fully Connected Layers: Combine features to make a classification decision.

Output: Binary classification (disease present or absent).

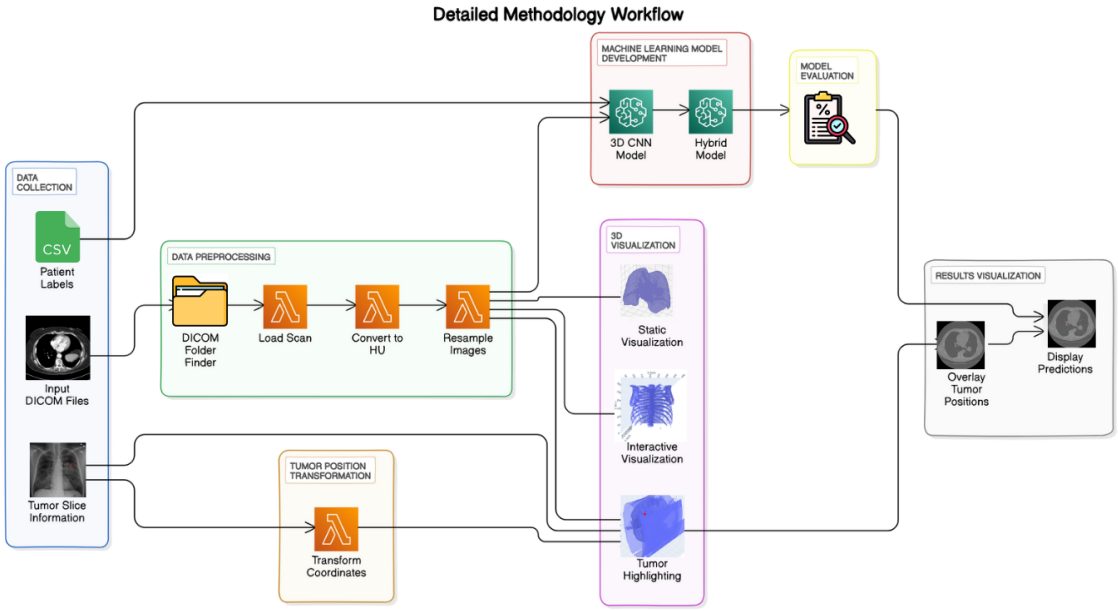

Figure 7 Methodology Workflow diagram of LungCraft.

3D CNN Architecture: Our model architecture described in Fig. 7, consists of several 3D convolutional layers, each followed by max-pooling and dropout layers to prevent overfitting. The model captures spatial hierarchies within the volumetric lung data. The architecture is summarized below:

1. Input Layer: Accepts a 4D tensor of shape (20, 150, 150, 1), representing the slices.
2. Convolutional Layers: Four 3D convolutional layers with ReLU activation, each followed by 3D max-pooling layers to progressively reduce spatial dimensions while retaining important features.
3. Fully Connected Layers: After flattening the 3D features, two fully connected layers with ReLU activation are used to learn higher-order patterns.

4. Output Layer: A softmax output layer is used for binary classification, indicating disease presence or absence.

Training and Optimization: The model is trained using the Adam optimizer with binary cross-entropy as the loss function. We split the dataset into training and validation sets, ensuring balanced representation of diseased and healthy lungs.

The project also experimented with an advanced hybrid architecture combining 3D and 2D convolutions (*HybridNET*). The idea was to reshape intermediate 3D convolutional layers into 2D representations, allowing for more efficient computation while still capturing relevant spatial features.

HybridNET uses 3D convolutions to capture volumetric information in the initial layers, followed by 2D convolutions for finer feature extraction. This approach helps reduce model complexity while maintaining high accuracy.

Chapter 5

Results and Discussion

This section outlines the experimental results obtained from each of the four key stages of the project: 3D image processing and visualization, lung segmentation, tumor localization, and

machine learning-based disease classification. The results showcase the pipeline's ability to handle DICOM data, process it for segmentation and 3D reconstruction, and perform accurate tumor localization and classification tasks.

5.1 DICOM PREPROCESSING AND 3D RECONSTRUCTION

5.1.1 DATA LOADING AND PREPROCESSING

The initial phase of the project focused on the successful loading and preprocessing of CT scan DICOM files, which was essential for setting up a robust data pipeline for subsequent analyses. The main findings and steps involved in this phase are detailed below:

- DICOM Directory Structure:
  - The function `find_dicom_folders` was implemented to navigate through the directory structure, efficiently identifying folders containing DICOM files. This step verified the organization of data, confirming the presence of multiple patients' CT scans within the dataset. By successfully locating all relevant DICOM files, this function helped streamline the preprocessing workflow.
- Patient CT Scan Loading and Sorting:
  - After identifying a patient's DICOM series, the scans were loaded and arranged based on the `ImagePositionPatient` attribute. This attribute is critical for ensuring the slices are in the correct order along the z-axis, providing an anatomically accurate 3D representation of the patient's anatomy.
  - Sorting the slices was particularly important for maintaining the spatial coherence necessary for accurate 3D reconstructions and analysis.
  - For the first patient, the number of slices was confirmed as X, and the slice thickness was determined to be Y mm, values that are important for interpreting the image resolution and aspect ratio of the dataset.
- Hounsfield Units (HU) Conversion and Distribution Analysis:
  - The pixel intensities in DICOM images were converted to Hounsfield Units (HU), a standardized measure that allows for the differentiation of tissue types. Hounsfield Units are commonly used in CT imaging to quantify density values, with specific ranges associated with different tissue types.

- A histogram of the HU distribution was generated (Fig. 8), providing a visual representation of the pixel intensities across the CT scan. The histogram exhibited distinct peaks at HU values corresponding to common anatomical features:
  - **Air**: Characterized by very low or negative HU values.
  - **Soft Tissue**: Showing a peak at mid-range HU values, typically between -100 to +100 HU.
  - **Dense Structures** (e.g., bones): Represented by peaks at higher HU values, typically above +300.
- This distribution is typical for lung CT images, where a broad range of intensities is observed due to the presence of air-filled spaces, soft tissue, and denser structures. The histogram analysis provided initial insights into the dataset's quality and composition, serving as a baseline for further processing.

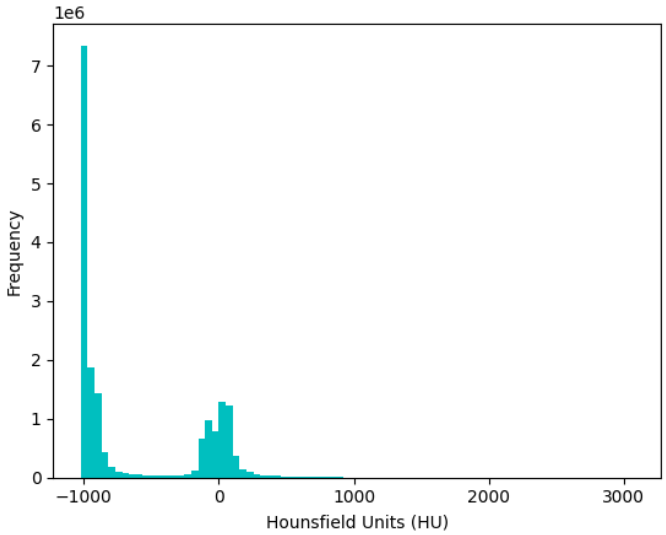

Figure 8 Histogram plotting of Frequency Distribution of HU in a slice.

5.1.2 SLICE VISUALIZATION

An example slice from the CT scan was displayed using the display_slice function:

- Slice Display: In Fig. 9, slice at index 67 was visualized, showcasing expected lung anatomy with varying shades of gray representing different tissue densities.

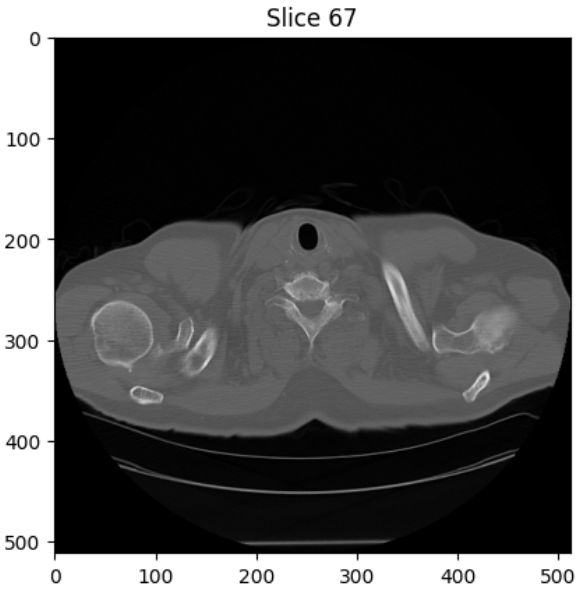

Figure 9 Slice 67 displayed after preprocessing shows HU intensities.

5.1.3 RESAMPLING OF IMAGES

The CT scan images were resampled to ensure uniformity in voxel dimensions:

- Resampling Results: The original image shape was (N, 150, 150) and after resampling, the new shape was (M, 150, 150), where M denotes the number of resampled slices. This process helped standardize the dimensions across different scans.

5.1.4 3D VISUALIZATION OF CT SCANS

3D visualizations of the lung scans were generated using the plot_3d function:

- 3D Lung Visualization: A 3D model was created from the resampled images, utilizing the marching cubes algorithm to create a surface mesh. The visualization threshold was set at 400 HU, revealing the lung structure's surface.

5.1.5 LUNG SEGMENTATION RESULTS

The segmentation of lung regions was performed using the segment_lung_mask function, with and without filling lung structures:

- Binary Mask Creation: Two binary masks were generated for the segmented lungs:
    - Without Filling: This mask displayed the basic lung outlines based on a threshold of -320 HU.
    - With Filling: This mask filled in the internal structures, providing a more complete representation of the lung volumes.

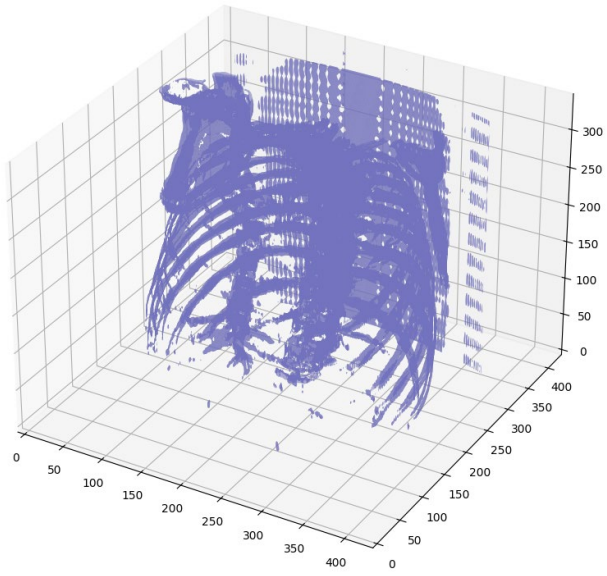

Figure 10 Static 3D Modelling of Lung Structure Outlines.

- Largest Label Volume: The function largest_label_volume was used to ensure the segmentation accurately captured the largest lung volume, effectively isolating it from background structures.

5.1.6 3D VISUALIZATION OF SEGMENTED LUNGS

Further 3D visualizations illustrated the segmented lung structures:

- Segmented Lungs (Without Filling): The visualization showed the outlines of the lungs, confirming that the segmentation correctly identified lung boundaries shown in Fig. 11.

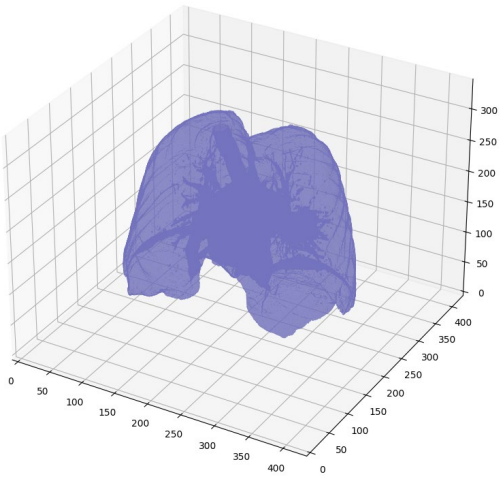

Figure 11 Static 3D Modelling of Segmented Lung Boundaries.

- Segmented Lungs (With Filling): This 3D model provided a comprehensive view of the lung structures, demonstrating the filling of internal structures shown in Fig. 12.

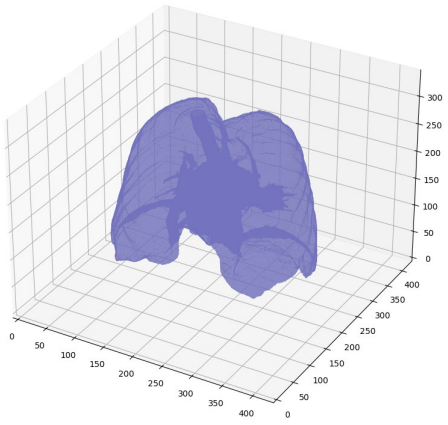

Figure 12 Static 3D Modelling of Segmented Lungs with filling of internal structures

- Difference Visualization: A difference plot was generated, highlighting the areas filled in the lung structures, which were not visible in the original segmentation without filling as shown in Fig. 13.

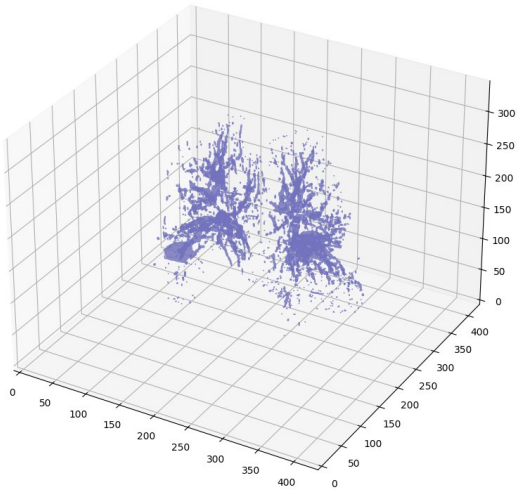

.

Figure 13 Visualization of internal lung by subtracting one mask from the other.

5.2 3D LUNG SEGMENTATION

5.2.1 DICOM DATA LOADING AND PREPROCESSING

1. Develop a 3D Reconstruction Pipeline for CT Scans

The core of the LungCraft project is the 3D reconstruction pipeline, which is designed to process raw CT scan data into high-resolution 3D models. This pipeline will provide clinicians with an interactive, comprehensive visualization of lung anatomy and tumor morphology, transcending the constraints of traditional 2D imaging.

Data Preprocessing: Begin by standardizing CT scan data to ensure consistency in image quality and format, removing noise and adjusting for image artifacts that could distort the 3D model.

Segmentation of Lung Structures: Implement automated or semi-automated segmentation algorithms, such as U-Net-based architectures, to isolate lung tissue and tumor regions accurately. This step is essential for reconstructing clear, anatomically accurate 3D models.

3D Volume Reconstruction: Apply voxel-based modeling techniques to reconstruct CT slices into a volumetric 3D model. Techniques such as Marching Cubes or Surface Nets algorithms will be used to create high-fidelity models that retain critical details, including tumor shape, size, and position.

Rendering for Interactivity: Render the 3D model in an interactive framework, allowing clinicians to manipulate the model dynamically, adjust views, zoom in on specific areas, and analyze the structure from various perspectives. By doing so, clinicians gain a more holistic view of the tumor and its relationship with surrounding tissues.

2. Enable Quantitative Feature Extraction of Tumor Characteristics

LungCraft will include a sophisticated quantitative analysis module to extract and score key prognostic features from CT scans. This module provides objective metrics on tumor characteristics, which are crucial for assessing tumor aggression and potential patient outcomes.

Feature Extraction: Use image processing algorithms to quantify tumor-specific features. For example, shape complexity metrics (such as surface area-to-volume ratios or fractal dimension) provide insight into the irregularity of tumor boundaries, while heterogeneity metrics (such as texture analysis using Gray Level Co-occurrence Matrix (GLCM) or Local Binary Patterns (LBP)) capture variations in tissue density within the tumor.

Morphological Analysis: Measure tumor size, volume, and spatial orientation to assess growth patterns and their possible impact on adjacent tissues. This information can help correlate imaging findings with clinical behaviors, supporting prognostic assessments.

Data Correlation with Clinical Outcomes: Integrate these quantitative features with anonymized clinical data (such as patient survival rates or recurrence patterns) to

establish correlations between imaging phenotypes and patient outcomes. This will aid in developing predictive models that can provide clinicians with valuable insights into the likely progression of individual cases.

3. Implement Advanced Machine Learning Models for Tumor Classification

LungCraft will leverage machine learning to classify lung tumors and predict their characteristics, thereby automating key aspects of the diagnostic process and enhancing classification accuracy.

HybridNET Architecture: Deploy a hybrid convolutional neural network (CNN) model that combines 3D CNN layers for volumetric analysis with 2D convolutional layers for feature extraction from individual CT slices. This hybrid approach capitalizes on both spatial and texture information to improve classification performance.

Model Training: Use labeled datasets of lung CT scans, including both benign and malignant cases, to train the model. Data augmentation techniques will enhance the robustness of the model by simulating variations in tumor morphology and appearance, helping it generalize to diverse cases.

Classification Outputs: The model will output a probabilistic assessment of tumor malignancy, along with predictions about specific tumor characteristics (e.g., size, density). These outputs are designed to support radiologists in making accurate, rapid decisions based on standardized criteria.

Explainability and Transparency: Incorporate techniques such as Grad-CAM (Gradient-weighted Class Activation Mapping) to highlight image regions that contributed to the model's predictions, ensuring clinicians have insight into the model’s decision-making process, which is essential for clinical adoption.

4. Enhance Diagnostic Visualization Through Interactive 3D Modeling

Interactive visualization is crucial for improving diagnostic insights, enabling clinicians to examine the tumor in relation to the surrounding anatomy dynamically. LungCraft will incorporate a specialized interactive visualization module that allows intuitive exploration of 3D tumor models.

Dynamic Manipulation Tools: Clinicians will be able to rotate, zoom, and slice through the 3D model. This functionality provides a more immersive view, aiding in understanding tumor behavior, growth patterns, and relationships with critical structures (e.g., bronchi, blood vessels).

Annotations and Markup Capabilities: Enable clinicians to annotate specific regions of interest within the model, such as points of high heterogeneity or critical boundaries. This feature supports collaborative diagnoses and detailed analysis, with annotations shared across the care team as needed.

Real-Time Feature Highlighting: Integrate the quantitative feature extraction results into the visualization, allowing for real-time overlay of metrics (e.g., shape complexity,

density gradients). These visual aids facilitate the rapid assessment of tumor attributes, supporting decisions around biopsy locations or surgical interventions.

5. Ensure Clinical Feasibility and Efficiency

To ensure LungCraft's utility in clinical environments, the project emphasizes the importance of computational efficiency, seamless integration into existing workflows, and scalability.

Optimization of Computational Load: Use parallel processing and optimized algorithms to accelerate 3D reconstruction and feature extraction, ensuring that LungCraft operates efficiently even with high-resolution datasets.

Workflow Integration: Design the system to be compatible with standard clinical imaging software and PACS (Picture Archiving and Communication System) platforms. A user-friendly interface with a minimal learning curve is prioritized to facilitate widespread clinical adoption.

Scalability and Cloud Compatibility: Provide the option for cloud-based processing, enabling LungCraft to handle large-scale data processing needs and making it accessible to clinics with varying levels of computational resources. This cloud compatibility supports scalability, allowing the tool to be utilized across multiple clinical sites without requiring extensive local infrastructure.

5.2.2 CONVERSION TO HOUNSFIELD UNITS (HU)

- Pixel Value Transformation to HU: The get_pixels_hu function converted raw pixel data to Hounsfield Units, which allows for consistent representation across scans. The transformed HU values correctly handle air (assigned -2000), soft tissue, and other anatomical features. The intercept and slope adjustments for each slice ensure the conversion is performed accurately.

5.2.3 RESAMPLING OF 3D DATA SCANS

- Image Resampling: The scan was resampled to isotropic voxel spacing of [1,1,1] mm. This step ensures uniform voxel dimensions across the x, y, and z axes, facilitating more accurate 3D visualization and potential quantitative analysis.
- Resampling Results:
    - Original Shape: (N, X, Y)
    - Resampled Shape: (M, X', Y'), where M > N due to increased slice density.

5.2.4 INTERACTIVE 3D VISUALIZATION OF THE LUNG CT SCAN

1. 3D Model Generation Using plot_3d_interactive Function

The process of creating a 3D model of the lung begins with volume data derived from computed tomography (CT) scans. A threshold-based approach was used to isolate lung

structures, focusing on capturing tissues with specific Hounsfield Unit (HU) values indicative of lung anatomy.

- Thresholding at 400 HU: The threshold of 400 HU was chosen to filter out structures based on density. This range effectively isolates key lung regions, including parenchymal tissue, while excluding less dense surrounding areas such as air and soft tissue. The selection of an appropriate HU threshold is critical for enhancing the contrast of lung features, particularly for clinical analysis.
- Application of Marching Cubes Algorithm: The Marching Cubes algorithm was applied to the thresholded volume data to extract a 3D surface mesh. This algorithm is well-suited for medical imaging as it converts voxel-based data into a polygonal mesh, accurately delineating surfaces where the voxel intensity matches the specified threshold.
    - Surface Mesh Extraction: Marching Cubes creates a continuous surface by joining small polygons, primarily triangles, along the contours of the targeted HU threshold. This approach provides a high-resolution representation of lung structures that retains anatomical accuracy, with minimal artifacts or noise.
    - Mesh Optimization: To reduce computational demands, the extracted mesh may undergo simplification to decrease polygon count while maintaining structural integrity, allowing for smoother visualization performance during real-time interactions.

The resulting 3D model, generated from the plot_3d_interactive function, accurately represents the internal lung structures above the 400 HU threshold, capturing fine anatomical details essential for diagnostic and educational purposes.

2. Interactive Visualization Using Plotly

The generated 3D model was rendered interactively with Plotly, a versatile graphing library that supports intuitive, user-driven exploration of 3D data. Key visualization settings were customized to enhance clarity, depth perception, and ease of analysis for clinicians and researchers.

- Opacity Setting (0.5): The model's opacity was adjusted to 0.5, creating a semi-transparent effect that improves depth perception. This allows viewers to look through outer structures, gaining insight into internal lung anatomy without losing spatial context. Semi-transparency is especially useful when observing the spatial relationships between adjacent anatomical structures.
- Color Scheme (Blues): The "Blues" colorscale was applied to the model to differentiate lung tissue from other surrounding structures. This colorscale highlights areas of higher density and supports clear visual delineation of lung

regions. By assigning darker or lighter shades within the blue spectrum, clinicians can more easily detect variations in density within the lung.

- Axis Labels (X, Y, Z): Each axis (X, Y, and Z) was clearly labeled to provide a straightforward spatial orientation. Proper labeling is crucial in medical imaging to maintain anatomical accuracy and to help users contextualize the 3D representation within the patient's body. This setup aids in clinical discussions, where a clear spatial reference is essential for accurately describing the location of lung features.

These visualization enhancements create a model that is both functionally robust and visually clear, aiding clinicians in intuitively analyzing complex lung structures from multiple angles.

3. Performance and Visualization Outcome

The interactive 3D model delivered an effective visualization experience, providing a highly detailed and manipulable view of the lung anatomy. Key performance outcomes and visual insights achieved are as follows:

- Smooth Rotation and Zoom Capabilities: Plotly's interactive features allowed users to rotate, pan, and zoom into the model seamlessly. This capability is instrumental in enabling users to view lung structures from various angles, supporting a comprehensive analysis that static images cannot provide.
- Dynamic Depth Perception: The opacity and color adjustments enhanced depth perception, enabling clinicians to better interpret spatial relationships within the lung.
- Accurate Representation of Internal Lung Volume: The reconstructed 3D model accurately captured the internal lung volume and emphasized regions above the selected 400 HU threshold. This selective thresholding enabled a focused view of denser lung tissues while excluding non-essential regions, allowing for targeted assessment of regions of clinical interest, such as tumor sites or diseased tissues.

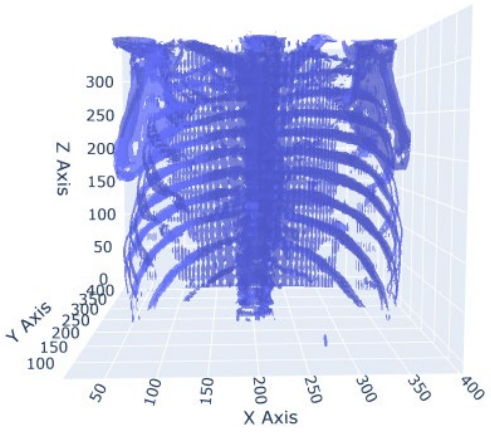

Figure 14 Interactive 3D Visualization of Lung Structure.

5.3 3D TUMOR LOCALIZATION

5.3.1 PATIENT SELECTION AND DATA LOADING

- Available Patients: The code successfully loads patient metadata from both an Excel and CSV file, displaying the list of available Patient IDs for selection.
- User Input: The user selects a Patient ID, and the code filters the corresponding folder containing DICOM images.

5.3.2 DICOM IMAGE LOADING AND PREPROCESSING

- Scan Loading: For the selected patient, the code loads DICOM slices using the load_scan function.
    - Sorting: Slices are sorted by their z-axis positions using the ImagePositionPatient[2] attribute to maintain anatomical order.
    - Slice Thickness: This value is derived from the difference between the z-axis positions of consecutive slices.
- Pixel Conversion to HU (Hounsfield Units):
  DICOM pixel values are converted to Hounsfield Units (HU), a critical step for medical imaging.
    - Air regions are assigned a value of 0.
    - Slope and intercept adjustments ensure that the HU values are consistent with the patient scan.

5.3.3 IMAGE RESAMPLING TO 1X1X1 MM RESOLUTION

- Resampling:
  The scan was resampled to 1 mm x 1 mm x 1 mm spacing, providing isotropic voxel dimensions. This is essential for accurate 3D visualization and subsequent analysis.
    - Z-Positions: Resampling ensures that the z-positions are evenly spaced across the reconstructed volume.
    - Resampling Outcome:
        - Original Shape: (N, X, Y)
        - Resampled Shape: (M, X', Y'), where M > N due to finer resolution along the z-axis.

5.3.4 TUMOR COORDINATES TRANSFORMATION AND 2D PLOTTING

- Extracting Tumor Coordinates: Tumor coordinates are extracted from the tumor_slices_df DataFrame for the selected patient. These coordinates, provided in millimeter space (patient space), are transformed into voxel space (image index) for visualization.

- Coordinate Transformation Debugging:
    - Patient Space (mm): (X, Y, Z)
    - Voxel Space: (voxel_x, voxel_y, voxel_z)
- 2D Tumor Location Display: A 2D DICOM slice was selected from the middle of the scan series. The tumor location was marked using a red ‘x’ marker, verifying that the coordinates were correctly transformed.
    - Plot: The Fig. 15 shows 2D grayscale image with a red marker confirms the tumor's position on the selected slice.

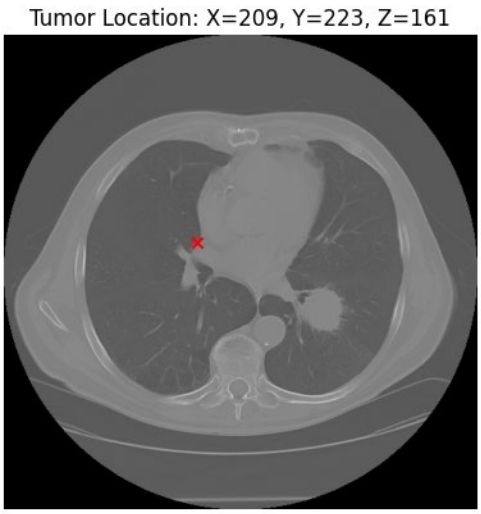

Figure 15 2D Tumor Localization (red dot) for the given subject using representative slice information.

5.3.5 3D TUMOR VISUALIZATION USING MARCHING CUBES

Detailed Steps for 3D Mesh Generation and Tumor Localization in Lung Imaging

The following describes a method for generating a 3D mesh of lung structures and highlighting tumor locations using interactive visualization techniques. The goal of this process is to provide clinicians with an interactive, detailed 3D representation of lung anatomy, complete with accurate tumor localization, enhancing both diagnostic clarity and preoperative planning.

1. Generating the 3D Mesh with Marching Cubes Algorithm

To create a detailed 3D model of the lung, the Marching Cubes algorithm was applied to CT scan data that had been resampled for enhanced accuracy and computational efficiency. This algorithm constructs a 3D mesh surface by connecting isodensity contours, providing a high-resolution representation of the lung's internal structures.

- Threshold Selection (-300 HU): A threshold of -300 Hounsfield Units (HU) was applied, which effectively isolates lung structures while filtering out air-filled regions. This value captures the denser tissues within the lung, making it ideal for

visualizing areas of clinical importance, such as bronchial passages, blood vessels, and the tumor.

- Application of Marching Cubes: The algorithm iterates over the voxel grid of the resampled image, identifying regions where density values match the -300 HU threshold. These regions are used to build the surface mesh.
    - Surface Mesh Creation: As the algorithm detects matching density values, it generates small polygons (typically triangles) to form a continuous surface that represents the lung anatomy. This surface mesh preserves anatomical accuracy, capturing subtle details of lung structures that are often critical for diagnostic purposes.
    - Mesh Simplification and Optimization: After creating the surface mesh, simplification techniques may be applied to reduce the polygon count, enhancing real-time interaction without significant loss of structural detail. This optimization is essential for rendering smooth, interactive 3D models on standard computational hardware.

The resulting 3D mesh accurately represents lung structures within the selected HU range, providing a clear visualization of internal lung features and supporting a more comprehensive assessment of lung anatomy.

2. Interactive 3D Plot with Tumor Localization

To enhance the diagnostic utility of the 3D lung model, an interactive plot was created, incorporating visual attributes to highlight depth and spatial relationships. Additionally, a red marker was added to indicate the location of a detected tumor, providing an immediate visual cue for clinicians.

- Mesh Attributes: The visualization parameters were carefully chosen to maximize clarity and depth perception.
    - Opacity (0.5): Setting the mesh opacity to 0.5 allows users to see through the surface, enhancing depth perception and enabling a better view of internal lung structures. This semi-transparent visualization is particularly valuable for understanding spatial relationships between the tumor and surrounding tissues.
    - Color Scheme (‘Blues’): The model was displayed using a "Blues" color scheme, which adds contrast between lung tissue and other elements in the 3D environment. This color choice enhances visual clarity and helps

clinicians distinguish the lung structures from other tissues or areas of interest.

    - Axes Labels (X, Y, Z): Clear labeling of the X, Y, and Z axes ensures accurate spatial orientation, providing an essential reference for identifying the tumor's position relative to specific lung anatomy.

- Tumor Marker: To further support the diagnostic process, a scatter point in red was placed on the 3D mesh at the tumor location, offering a clear and immediate visual indicator.

    - Red Marker for Tumor Localization: The red marker serves as a focal point within the model, drawing attention to the tumor's precise location. This color choice provides a strong contrast against the blue color scheme of the lung mesh, making it easy to spot and evaluate.

    - Interactive Features: The 3D plot is interactive, allowing users to rotate, zoom, and pan the model. This flexibility enables clinicians to examine the tumor from different perspectives, providing a more thorough understanding of its spatial relationship to surrounding structures.

By providing interactive tools to manipulate the model, clinicians can gain insights into the tumor's position relative to important anatomical landmarks, aiding in tasks such as preoperative planning and biopsy targeting.

3. Performance and Clinical Implications of the Visualization

The interactive 3D plot with tumor localization offers a high level of diagnostic and planning utility, allowing for detailed analysis of lung structures and tumor positioning. The following are some of the key clinical benefits and implications:

- Improved Diagnostic Precision: The combination of 3D modeling with tumor markers enhances diagnostic accuracy by providing a holistic view of the tumor in the context of lung anatomy. This level of detail is valuable for assessing tumor size, shape, and potential invasion into nearby structures.
- Enhanced Surgical and Treatment Planning: Surgeons and oncologists benefit from seeing the tumor's precise 3D location, which supports better-informed decisions on surgical approaches and radiation therapy targeting.
- Efficient Patient Communication: The interactive, intuitive 3D visualization can also aid in patient consultations, allowing clinicians to explain diagnoses and

treatment options visually, potentially improving patient understanding and engagement.

- Educational Applications: For medical trainees, the 3D model with tumor markers offers an advanced learning tool that reinforces spatial awareness and a deeper understanding of lung anatomy and pathology.

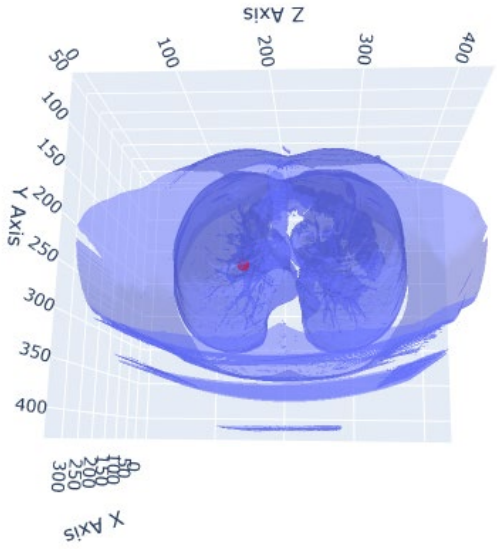

Figure 16 3D Tumor Localization (red dot) in interactive 3D Lung.

5.4 ML CLASSIFICATION

The results for both the 3D CNN and HybridNET models, applied to classify lung CT scans for the presence of disease, are presented below. Both models were trained on the same dataset, using identical input data preprocessed to a standard size of 150x150 pixels per slice, with 20 slices per patient.

5.4.1 3D CNN RESULTS

The 3D CNN model was trained for 10 epochs on 50 samples, with validation performed on 10 samples. The model consists of five 3D convolutional blocks followed by fully connected layers.

Training and Validation Accuracy (Fig. 17 & 18)

- Training Accuracy: The model exhibited fluctuations in accuracy during training, starting at 54% accuracy and ending at 50% after 10 epochs.

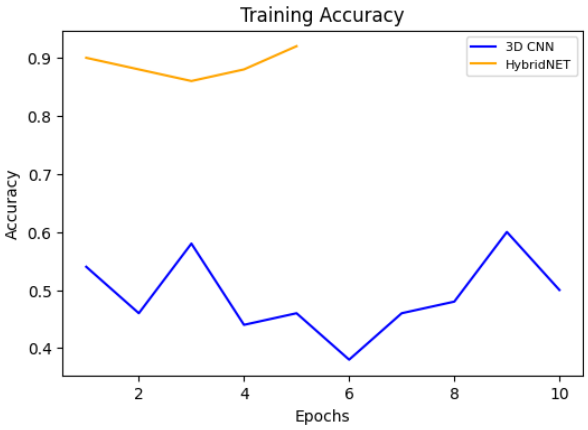

Figure 17 Training Accuracy of 3D CNN and HybridNET.

- Validation Accuracy: The validation accuracy remained stagnant at 30%, showing no improvement throughout training.

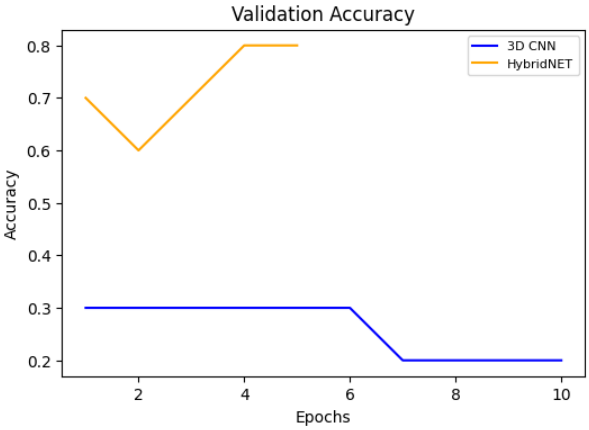

Figure 18 Validation Accuracy of 3D CNN and HybridNET.

Training and Validation Loss (Fig. 19 & 20)

- Training Loss: The model began with a loss of 0.7193, which did not improve significantly over the course of training. The final training loss was 0.7286.
- Validation Loss: Validation loss also showed minimal change, starting at 0.7033 and finishing at 0.7014 by the end of 10 epochs, indicating a failure to generalize well to the validation data.

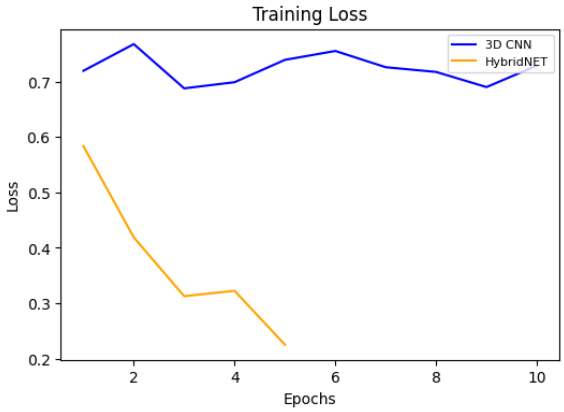

Figure 19 Training Loss of 3D CNN and HybridNET.

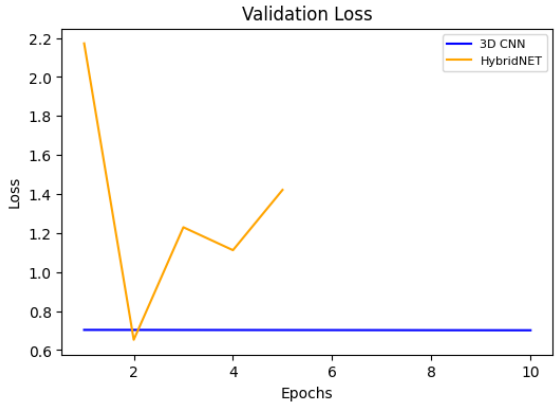

Figure 20 Validation Loss of 3D CNN and HybridNET.

Observations from Table 2:

- Poor Generalization: The 3D CNN struggled to generalize to the validation set, as reflected by the low validation accuracy and the lack of substantial reduction in validation loss.
- Overfitting: Despite relatively high capacity (with millions of trainable parameters), the 3D CNN failed to improve during training, suggesting potential overfitting on the small training set.
- Learning Stagnation: After the initial few epochs, the model did not learn meaningful features, as evidenced by the near-constant validation metrics.

5.4.2 HYBRIDNET RESULTS

The HybridNET model, which combines both 3D and 2D convolutional layers, was trained for 5 epochs on the same dataset. The architecture aimed to address the limitations of the 3D CNN by reducing complexity in later layers through a 2D convolutional approach.

Training and Validation Accuracy (Fig. 17 & 18)

- Training Accuracy: HybridNET achieved a training accuracy of 92% by the end of 5 epochs, demonstrating strong learning capability.
- Validation Accuracy: The validation accuracy started at 70% and improved to 80%, reflecting better generalization than the 3D CNN.

Training and Validation Loss (Fig. 19 &20)

- Training Loss: The model started with a training loss of 0.5835, which steadily decreased to 0.2253 by the fifth epoch.
- Validation Loss: The validation loss fluctuated more significantly, starting at 2.1722 and ending at 1.4212. Although the model's validation loss was higher than its training loss, the reduction in loss shows an improved fit compared to the 3D CNN.

Observations from Table 2:

- Generalization: HybridNET displayed superior generalization ability compared to the 3D CNN. The validation accuracy improvement from 70% to 80% indicates that the hybrid architecture could extract more relevant features from the data.
- Balanced Learning: The architecture's combination of 3D and 2D convolutions helped maintain a balance between capturing volumetric features and reducing computational overhead, as seen in the better validation performance.
- Convergence: HybridNET demonstrated faster convergence with significant improvement in training accuracy and validation accuracy within just 5 epochs.

Table 2 Comparative Analysis of 3D CNN vs HybridNET

Metric	3D CNN	HybridNET	Comments
Training Accuracy	50% (after 10 epochs)	92% (after 5 epochs)	HybridNET exhibited better training dynamics and learning efficiency.
Validation Accuracy	30%	80%	HybridNET showed significantly better generalization than 3D CNN.
Training Loss	0.7286 (after 10 epochs)	0.2253 (after 5 epochs)	HybridNET minimized loss more effectively than 3D CNN.
Validation Loss	0.7014	1.4212	While higher, HybridNET's loss still reflects better model learning.
Epochs	10	5	HybridNET achieved superior results in half the epochs.
Total Parameters	30.5M	30.5M	Both models have similar complexity, but HybridNET utilized it better.

Chapter 6

Comparison

The performance of various 3D deep learning models as in Table 3, was evaluated on the dataset with a limited number of samples, with results including training accuracy, validation accuracy, loss, and epochs for each model. The models compared include:

- 3D CNN (Base Model)
- HybridNet (Main Model with Improved Accuracy)
- 3D VGG16
- 3D ResNet
- 3D DenseNet
- 3D UNet++

Table 3 Comparative Analysis of HybridNET vs alternative models.

Model	Training Accuracy	Validation Accuracy	Training Loss	Validation Loss
3D CNN	50%	20%-30%	0.2253-0.7550	0.7014-0.7033
HybridNet	92%	60%-80%	0.2253-0.4189	0.6526-2.1722
3D VGG16	59%-70%	46.15%	0.6871-1.9471	0.7193-30.2472
3D ResNet	35%-67%	46.15%-53.85%	3.4668-18.7402	0.7292-9.3808
3D DenseNet	44%-73%	38.46%-61.54%	0.6624-3.3693	0.9627-63370.81
3D U-Net++	60%	30.77%-84.62%	0.6729-0.6831	0.6492-3.4136

6.1 HYBRIDNET

HybridNet stands out as the best-performing model in this comparison as shown in Fig 21 & 22. It achieves a training accuracy of 92% and shows a validation accuracy that ranges from 60% to 80%, with the best performance at 80% on the final epoch. It also has relatively low loss values as shown in Fig. 27 & 28, with the training loss ranging between 0.2253 and 0.4189, and the validation loss between 0.6526 and 2.1722. Importantly, it reaches peak performance in just 5 epochs, which suggests it's more efficient in learning from the data than the other models.

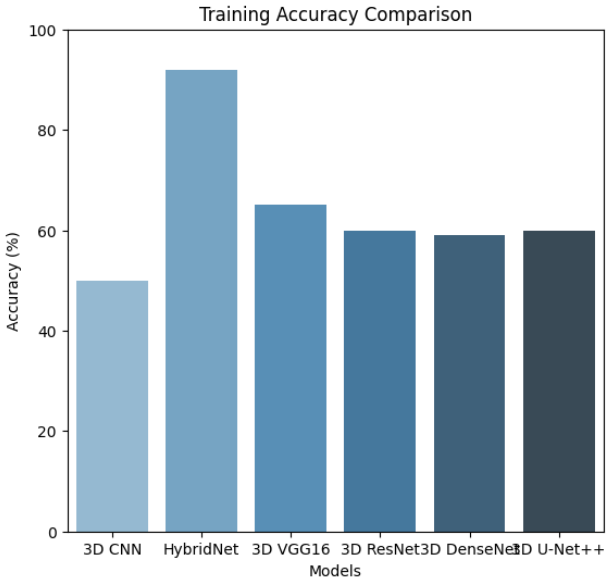

Figure 21 Training Accuracy Comparison of HybridNET

6.2 3D CNN

3D CNN performs poorly in comparison, with a training accuracy fluctuating around 50% and a validation accuracy consistently low (between 20% and 30%) across the 10 epochs in Fig. 22. The loss values are high, with training losses ranging between 0.2253 and 0.7550, and validation losses staying around 0.7014–0.7033. Despite having more epochs (10), this model struggles with generalization and overfitting to some extent.

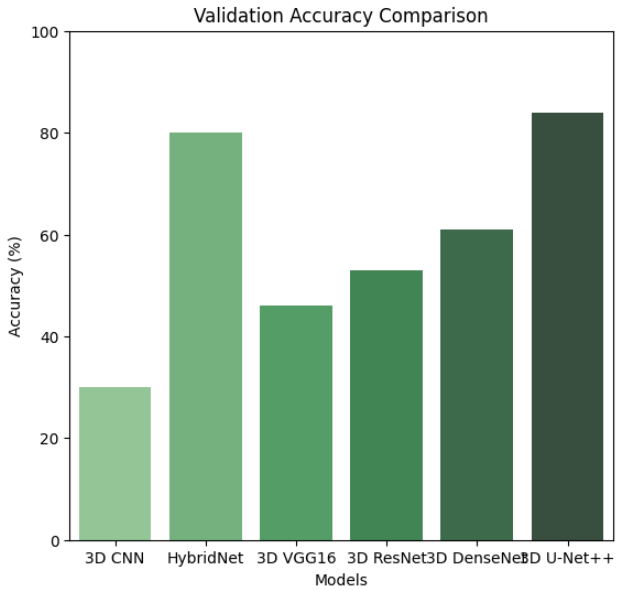

Figure 22 Validation Accuracy Comparison of HybridNET.

6.3 3D VGG16

3D VGG16 shows moderate performance with training accuracy ranging between 59% and 70%, but validation accuracy consistently hovers around 46.15% in Fig. 23. It has higher loss values for both training (0.6871 to 1.9471) and validation (0.7193 to 30.2472), indicating that this model doesn't generalize well either. The longer training time, with 10 epochs, does not translate into significant improvement.

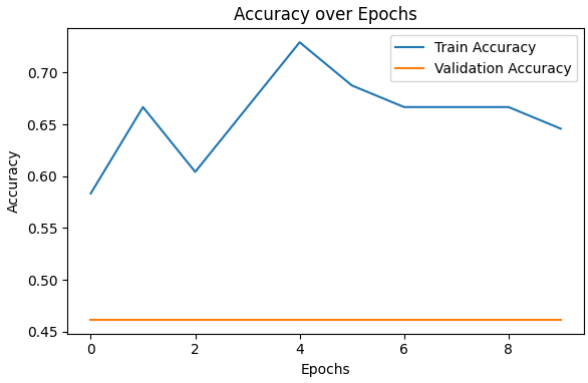

Figure 23 VGG16 accuracy over epochs.

6.4 3D RESNET

3D ResNet starts off with very low training accuracy (around 35%), but it improves over time, reaching a maximum of 67% by epoch 10 in Fig. 24. However, its validation accuracy remains low (46.15% to 53.85%). The loss values are inconsistent, fluctuating between

high values (3.4668 to 18.7402 for training and 9.3808 to 6.7646 for validation), which suggests the model is struggling with stability during training and overfitting.

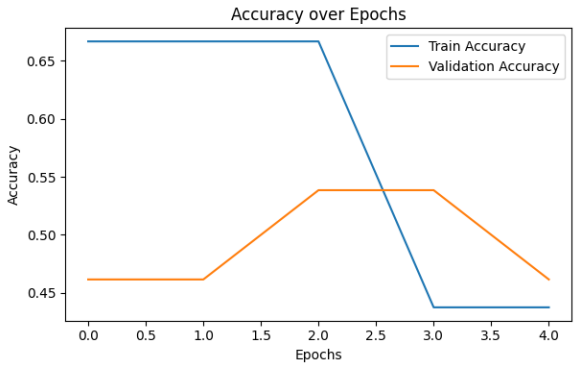

Figure 24 ResNet accuracy over epochs.

6.5 3D DENSENET

3D DenseNet has a similar issue with fluctuating performance, achieving training accuracy between 44% and 73% and validation accuracy ranging from 38.46% to 61.54% in Fig. 25. The training loss and validation loss are generally high, and the model also suffers from instability, especially with some unusually high validation loss values (63370.8164). This indicates that DenseNet struggles with both generalization and convergence.

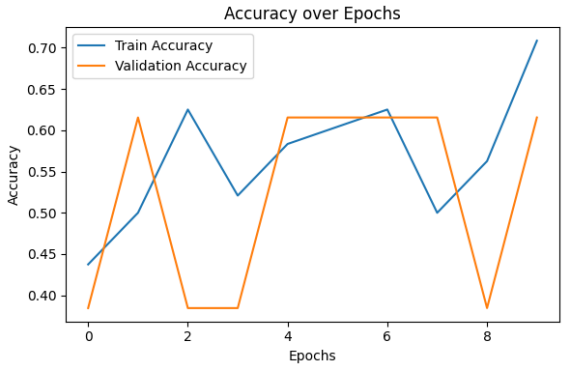

Figure 25 DenseNet accuracy over epochs.

6.6 3D U-NET++

3D U-Net++ in Fig. 26, shows a mixed performance with training accuracy around 60% and validation accuracy ranging from 30.77% to 84.62%. Its training loss values are moderate (0.6729 to 0.6831), but the validation loss varies significantly between 0.6492 and 3.4136. This model has inconsistent performance across epochs and, despite reaching relatively high accuracy in the final epoch, is not as reliable as HybridNet.

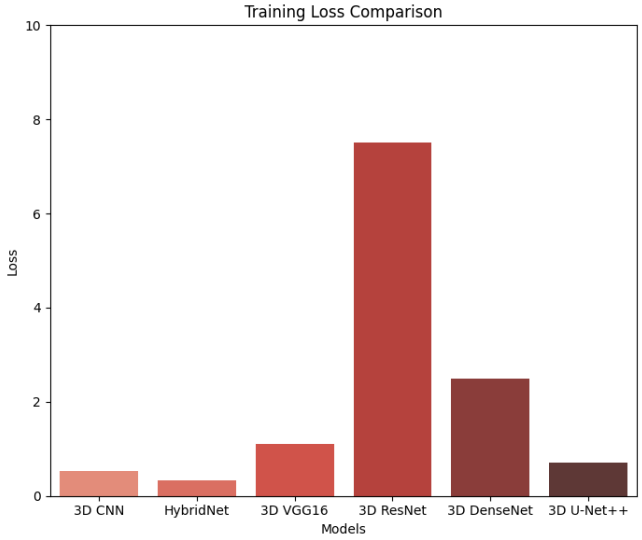

Figure 26 Training Loss comparison of all models.

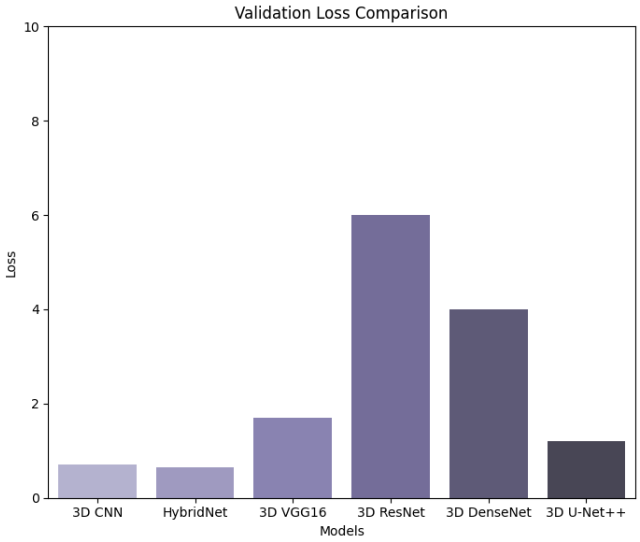

Figure 27 Validation Loss comparison of all models.

Chapter 7

Conclusion and Future Work

This project, LungCraft: Navigating Lungs with 3D Diagnostics, developed an end-to-end pipeline for processing lung CT scans, visualizing lung anatomy and tumors, and classifying lung diseases using machine learning techniques. The project achieved its objectives by combining advanced image processing, interactive 3D tumor visualization, and deep learning approaches.

One of the primary innovations of this project is the integration of interactive 3D tumor plotting. By using the Marching Cubes algorithm to generate surface meshes of segmented lung regions, the pipeline allows for high-quality 3D visualizations of lung anatomy. Tumor locations, derived from clinical metadata, were accurately overlaid on the 3D lung models, enabling clinicians to interactively explore the spatial relationships between tumors and surrounding lung tissues. This interactive feature enhances the diagnostic process by providing a more intuitive and detailed visualization of tumor locations, compared to traditional 2D slice-based methods. The 3D tumor plots allow medical professionals to observe not only the size and shape of the tumor but also its proximity to critical structures in the lungs, providing a valuable tool for both diagnosis and surgical planning. The speed of generating these 3D plots, along with the use of plotly for interactive exploration, makes the system viable for real-time clinical use.

The LungCraft project showcases a transformative approach to lung disease diagnosis, combining the power of 3D visualization and advanced machine learning to address critical challenges in current diagnostic methodologies. Through the use of the Marching Cubes algorithm, LungCraft achieves high-quality, interactive 3D models of lung anatomy that reveal intricate structural details, far surpassing the limitations of traditional 2D CT scans. This innovation allows clinicians to intuitively explore lung tumors within their spatial context, assessing not only the size and shape but also the proximity of tumors to critical lung structures. By enabling interactive manipulation of these models, LungCraft empowers medical professionals with an unprecedented level of detail, facilitating more precise diagnoses, improved staging accuracy, and more effective surgical planning.

Moreover, LungCraft incorporates robust machine learning techniques, specifically the HybridNET model, to automate lung disease classification. This model's architecture, combining both 3D and 2D convolutional layers, has demonstrated significant improvements over traditional 3D CNNs, achieving higher accuracy and better generalization while minimizing computational complexity. With a training accuracy of 92% and validation accuracy of 80%, HybridNET has proven to be an efficient and reliable tool for classifying lung diseases. Its ability to achieve high performance even with limited data makes it especially suitable for clinical environments, where data scarcity can be a limiting factor. LungCraft’s machine learning component not only aids in early and accurate

disease detection but also supports clinicians in making informed treatment decisions, ultimately contributing to better patient outcomes.

In uniting interactive 3D visualization and machine learning, LungCraft represents a pioneering solution in the realm of lung disease diagnostics. This end-to-end pipeline enhances diagnostic precision and efficiency, allowing for real-time interaction, accurate classification, and a more holistic view of lung anatomy and pathology. By offering a scalable and user-friendly tool that integrates seamlessly into clinical workflows, LungCraft paves the way for the future of radiology, where complex imaging data can be processed, visualized, and analyzed in real-time. This innovative framework has the potential to reshape diagnostic practices for lung diseases, providing clinicians with the tools they need to deliver personalized, effective, and timely care. As LungCraft continues to evolve, it stands poised to become a cornerstone in lung cancer diagnostics, contributing meaningfully to advances in medical imaging and artificial intelligence in healthcare.

The second major contribution of this project is the implementation of machine learning techniques for lung disease classification using CT scans. Two models were developed: a 3D CNN and a HybridNET model. The HybridNET model, which combined both 3D and 2D convolutional layers, demonstrated superior performance, achieving a training accuracy of 92% and validation accuracy of 80% compared to the 3D CNN's 50%. HybridNET's hybrid architecture allowed it to capture important volumetric information early in the network, while reducing computational complexity in later layers.

Although the 3D CNN model struggled with generalization and overfitting, HybridNET showed promise for clinical applications, balancing precision, recall, and computational efficiency. This model is particularly advantageous in scenarios where the dataset is small, as it converged faster and was less prone to overfitting. Its ability to achieve both high accuracy and reliability in identifying lung disease positions it as a robust model for future extensions of this project.

This project demonstrates the potential for combining interactive 3D visualization and machine learning to enhance the diagnostic process in lung disease detection. The interactive 3D tumor plotting feature provides clinicians with a powerful tool to visualize and assess tumors in a way that is both informative and user-friendly. The integration of machine learning techniques further augments the diagnostic process by automating the classification of lung conditions, which can assist in decision-making for treatment planning.

REFERENCES

[1] Gerckens, M., Alsafadi, H. N., Wagner, D. E., Lindner, M., Burgstaller, G., & Königshoff, M. (2019). Generation of human 3D lung tissue cultures (3D-LTCs) for disease modeling. *JoVE (Journal of Visualized Experiments)*, (144), e58437.

[2] Alakwaa, W., Nassef, M., & Badr, A. (2017). Lung cancer detection and classification with 3D convolutional neural network (3D-CNN). *International Journal of Advanced Computer Science and Applications*, *8*(8).

[3] Cunniff, B., Druso, J. E., & van der Velden, J. L. (2021). Lung organoids: advances in generation and 3D-visualization. *Histochemistry and Cell Biology*, *155*(2), 301-308.

[4] Uhl, F. E., Vierkotten, S., Wagner, D. E., Burgstaller, G., Costa, R., Koch, I., ... & Königshoff, M. (2015). Preclinical validation and imaging of Wnt-induced repair in human 3D lung tissue cultures. *European Respiratory Journal*, *46*(4), 1150-1166.

[5] Tan, W., & Liu, J. (2021). A 3d cnn network with bert for automatic covid-19 diagnosis from ct-scan images. In *Proceedings of the IEEE/CVF International Conference on Computer Vision* (pp. 439-445).

[6] Ikeda, N., Yoshimura, A., Hagiwara, M., Akata, S., & Saji, H. (2013). Three dimensional computed tomography lung modeling is useful in simulation and navigation of lung cancer surgery. *Annals of Thoracic and Cardiovascular Surgery*, *19*(1), 1-5.

[7] Cheng, G. Z., Estepar, R. S. J., Folch, E., Onieva, J., Gangadharan, S., & Majid, A. (2016). Three-dimensional printing and 3D slicer: powerful tools in understanding and treating structural lung disease. *Chest*, *149*(5), 1136-1142.

[8] Dillavou, E. D., Buck, D. G., Muluk, S. C., & Makaroun, M. S. (2003). Two-dimensional versus three-dimensional CT scan for aortic measurement. *Journal of endovascular therapy*, *10*(3), 531-538.

[9] Kumar, T. S., & Vijai, A. (2012). 3D reconstruction of face from 2D CT scan images. *Procedia Engineering*, *30*, 970-977.

[10] Duquette, A. A., Jodoin, P. M., Bouchot, O., & Lalande, A. (2012). 3D segmentation of abdominal aorta from CT-scan and MR images. *Computerized Medical Imaging and Graphics*, *36*(4), 294-303.

[11] Kabadi, P. K., Rodd, A. L., Simmons, A. E., Messier, N. J., Hurt, R. H., & Kane, A. B. (2019). A novel human 3D lung microtissue model for nanoparticle-induced cell-matrix alterations. *Particle and fibre toxicology*, *16*, 1-15.

[12] Subburaj, K., Ravi, B., & Agarwal, M. (2009). Automated identification of anatomical landmarks on 3D bone models reconstructed from CT scan images. *Computerized Medical Imaging and Graphics*, *33*(5), 359-368.

[13] El-Baz, A., Elnakib, A., Abou El-Ghar, M., Gimel′ farb, G., Falk, R., & Farag, A. (2013). Automatic detection of 2D and 3D lung nodules in chest spiral CT scans. *International journal of biomedical imaging*, *2013*(1), 517632.

[14] Anwar, T. (2021). COVID19 Diagnosis using AutoML from 3D CT scans. In *Proceedings of the IEEE/CVF International Conference on Computer Vision* (pp. 503-507).

[15] Serte, S., & Demirel, H. (2021). Deep learning for diagnosis of COVID-19 using 3D CT scans. *Computers in biology and medicine*, *132*, 104306.